NACA RM A57A10

NACA

RESEARCH MEMORANDUM

A WIND-TUNNEL INVESTIGATION OF THE EFFECTS OF CONICAL CAMBER FOR AN AIRPLANE CONFIGURATION HAVING A TRIANGULAR WING OF ASPECT RATIO 2.2

By E. Ray Phelps and John W. Boyd

Ames Aeronautical Laboratory
Moffett Field, Calif.

CLASSIFIED DOCUMENT

NATIONAL ADVISORY COMMITTEE FOR AERONAUTICS

WASHINGTON

April 30, 1957

NATIONAL ADVISORY COMMITTEE FOR AERONAUTICS

RESEARCH MEMORANDUM

A WIND-TUNNEL INVESTIGATION OF THE EFFECTS OF CONICAL CAMBER FOR AN AIRPLANE CONFIGURATION HAVING A TRIANGULAR WING OF ASPECT RATIO 2.2

By E. Ray Phelps and John W. Boyd

SUMMARY

19745

The results of an investigation directed at determining the effectiveness of various amounts and spanwise extents of conical camber on the aerodynamic characteristics of a wing-body-tail combination employing a triangular wing of aspect ratio 2.2 are presented. The surface shapes investigated were modifications of those derived from lifting surface theory for a Mach number of 1.0.

Five cambered wings were tested, all of which were designed for a Mach number of 1.0. The wings tested were cambered over the outboard 10 percent of the local semispan for design lift coefficients of 0.10 and 0.20 and over the outboard 15 percent of the local semispan for design lift coefficients of 0.10, 0.20, and 0.30. A plane wing was also tested to provide a basis for comparison. The lift, drag, and pitching moment were obtained for a Mach number range from 0.70 to 1.90 at a constant Reynolds number of 3.0 million and for angles of attack from -4° to $+12^{\circ}$.

The experimental results showed that a moderate amount of camber resulted in significant reductions of drag of the wing-body-tail combination at subsonic and transonic speeds; at low supersonic speeds, however, only small reductions of drag were realized. The use of greater amounts of camber produced large reductions in drag at lift coefficients above 0.20 for high subsonic and transonic speeds. At high supersonic speeds, however, the benefits of camber are considerably reduced and generally restricted to lift coefficients of 0.30 and above. Increase of the spanwise extent of the cambered area from 10 to 15 percent of the local semispan generally resulted in small reduction of the model drag for a design lift coefficient of 0.20. The lift and pitching moment were not significantly affected by the camber.

[redacted]

INTRODUCTION

One of the primary prerequisites in the design of an aircraft is the achievement of the lowest possible drag. For aircraft that fly at subsonic speeds this requires the minimization of the friction drag and of the drag due to lift. For airplanes that fly at supersonic speeds another source of drag must be considered - wave drag.

The present report presents the results of an experimental investigation directed at reducing the drag due to lift at subsonic and low supersonic speeds where it is largely vortex drag. It has been shown in reference 1 that a surface shape could be derived having aerodynamic characteristics which approximate the conditions necessary to attain the minimum vortex drag for triangular wings, namely, that the span load distribution approximate an ellipse and that the equivalent of the theoretical leading-edge thrust be realized. The experimental studies of references 1 and 2 show that a modification of the surface shape designated as conical camber resulted in large reductions in the drag due to lift values of such wings. The data also showed, however, that at supersonic speeds an increase in the drag near zero lift resulted from the camber. Subsequent studies have indicated that a smaller amount of camber than originally tested might be advantageous in that the zero-lift drag penalties would be reduced at supersonic speeds with little detriment to the drag reductions at subsonic speeds.

A study was undertaken, therefore, to determine the effectiveness of various amounts and extents of conical camber on the aerodynamic characteristics of a low-aspect-ratio triangular wing. The tests were conducted on a model of a fighter airplane having an aspect-ratio-2.2 wing of triangular plan form conically cambered over two different spanwise extents for several design lift coefficients. The present paper presents a comparison of the experimental data obtained for the model with the plane and cambered wings. Some comparisons are also made between experimental drag results and the theoretical values obtained for full and no leading-edge suction.

SYMBOLS

a ratio of the slope of a ray from the wing apex defining the inboard extent of the camber to the slope of the wing leading edge

b local span, measured at a streamwise station x

[redacted]

c	local chord, measured at a spanwise station y
$\bar{c}$	mean aerodynamic chord
c_l	section lift coefficient, $\frac{\text{section lift}}{qc}$
c_r	root chord
C_D	drag coefficient, $\frac{\text{drag}}{qS}$
C_{D_0}	drag coefficient of plane wing at zero lift
ΔC_D	increment in drag coefficient due to camber (drag coefficient of cambered wing minus drag coefficient of plane wing) for constant lift coefficient
C_L	lift coefficient, $\frac{\text{lift}}{qS}$
C_{L_d}	design lift coefficient
$C_{L_{opt}}$	lift coefficient for maximum $\frac{L}{D}$
C_m	pitching-moment coefficient, $\frac{\text{pitching moment}}{qS\bar{c}}$, referred to an axis $0.016\bar{c}$ above the lateral axis which passes through the mean aerodynamic chord at $0.275\bar{c}$
$\frac{L}{D}$	lift-drag ratio, $\frac{C_L}{C_D}$
$\left(\frac{L}{D}\right)_{max}$	maximum lift-drag ratio
m	slope of wing leading edge, cot Λ
M	free-stream Mach number
q	free-stream dynamic pressure
S	plan-form area of wing, including that portion within the body formed by extending the leading and trailing edges to the plane of symmetry
x,y,z	Cartesian coordinates in streamwise, spanwise, and vertical directions, respectively (The origin is at the wing apex.)
α	angle of attack of wing root chord, deg
Λ	angle of sweepback of wing leading edge, deg

[redacted]

THEORETICAL CONSIDERATIONS

In the theoretical development of reference 1, it was shown that a conically cambered surface shape could be derived which satisfied the two requirements necessary to the attainment of low drag due to lift for wings having subsonic leading edges, namely, that the span load distribution approximate an ellipse and that the equivalent of the theoretical leading-edge thrust be developed. The theoretically derived camber extended over the entire wing; however, as shown in reference 1, most of the camber was confined to the outboard sections of the wing. It was concluded therefore that, in order to simplify construction, the wing could be made planar over the inboard 80 percent of the local semispan without significantly altering the spanwise load distribution or adversely affecting the development of the equivalent thrust force. This was verified experimentally in reference 2 wherein it was shown that at subsonic speeds the wings incorporating the modified conical camber realized essentially the drag due to lift associated with a plane wing having elliptical span load distribution and full leading-edge suction.

In the design of aircraft the extent of the wing which can be cambered is often limited by structural considerations, so that it is of interest to determine the effects of various extents and degrees of conical camber. The wings utilized for the present investigation, therefore, contained modifications in addition to those described above to permit variation of the extent and degree of camber. The degree of camber or displacement of the wing leading edge was obtained directly from the design charts of reference 2 for the proper design lift coefficient and Mach number. Since it was desired to camber over smaller percents of the semispan than the 0.20 value for which the design charts of reference 2 were derived, an approximation to the shape of the camber line was necessary. A parabolic variation of the camber line was arbitrarily chosen from the wing leading edge to the inboard extent of the camber and is shown in figure 1. Also shown in figure 1 for comparison are the ordinates of the modified theoretical surface as obtained from the design charts of reference 2 for a design Mach number of 1.0. The parabolic camber line had as its vertex the point of tangency of the cambered surface and the plane surface and is defined by the equation shown in figure 1 for a design Mach number of 1.0. Since the basic requirement necessary to the attainment of the equivalent leading-edge thrust force, that is, that the wing leading edge be cambered, has not been invalidated by these modifications, it is reasonable to expect that an effective force in the thrust direction would still be realized. The question arises, however, as to what effect these modifications would have on the other requirement, the span load distribution. An analysis based on the linear lifting surface theory was made, therefore, to determine the span loading for the precise wing shapes that were tested. The

[redacted]

results of this study are shown in sketch (a) where it can be seen that the theoretical span loading for the wings cambered over both 10 and 15 percent of the semispan are not greatly different from the elliptical. It would be expected, therefore, that at the design conditions the drag due to lift of the wings with a parabolic variation of the camber line would closely approximate the minimum drag due to lift for a wing of this aspect ratio.

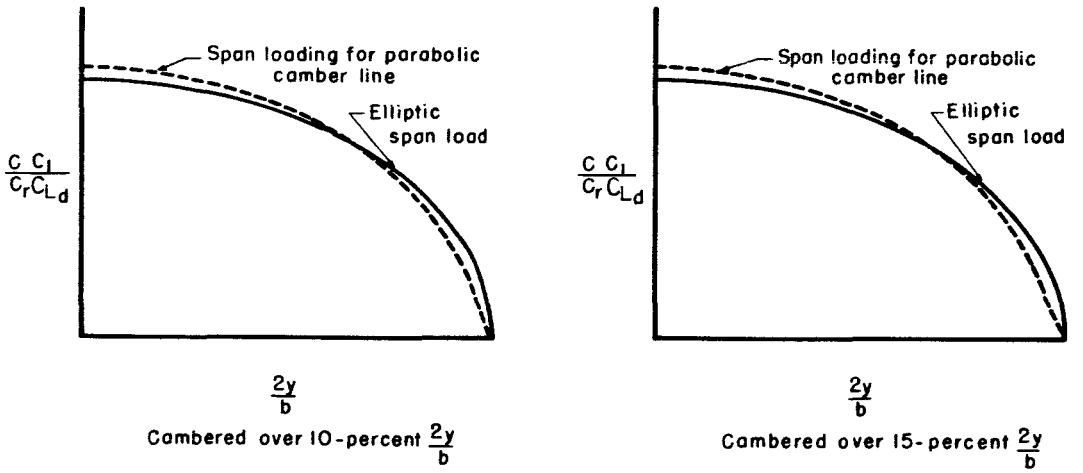

Sketch (a)

APPARATUS AND MODELS

Test Facility

The experimental studies reported herein were conducted in the Ames 6- by 6-foot supersonic wind tunnel, which is of the closed-circuit, variable-pressure type utilizing an asymmetric adjustable nozzle to obtain a Mach number range continuous from 0.7 to 2.2. The transonic capabilities are the result of recent modifications providing perforated upper and lower test-section walls. A part of the boundary layer is removed through the perforations to improve the stream characteristics. An upward extension of the Mach number range was obtained by the use of injector flaps downstream of the test section to reduce the required compression ratio across the nozzle and to better match the weight flow characteristics of the nozzle to those of the compressor.

An extensive survey of the wind-tunnel stream characteristics was undertaken upon completion of the modifications. Analysis of the results of the survey, although incomplete, are sufficiently advanced to establish the fact that the stream imperfections do not affect the validity of the results of the present investigation.

[redacted]

Description of Models

The present research program was directed primarily to the investigation of the effects of various amounts and extents of conical camber on the drag characteristics of a wing of triangular plan form. For this purpose a complete configuration comprising a triangular wing, indented body with open inlets, and a vertical tail, similar to that of a contemporary fighter airplane was used. Figures 2 and 3 show the test model. The triangular wing, which was of aspect ratio 2.2, was fitted with removable leading edges in order to permit rapid changes in the amount of camber. The wing area, leading-edge sweep, and aspect ratio were unchanged by the camber modifications to the leading edge.

Five cambered wings, all of which were designed for a Mach number of 1.0, were tested. Two of the wings incorporated camber over the outboard 10 percent of the local semispan and three incorporated camber over the outboard 15 percent of the local semispan. The degree of camber incorporated over the outboard 10 percent corresponded to design lift coefficients of 0.10 and 0.20. The degree of camber incorporated over the outboard 15 percent corresponded to design lift coefficients of 0.10, 0.20, and 0.30. The design of each of the cambered surfaces conformed with the method described under "Theoretical Considerations." A plane wing was also tested to provide a basis for comparison. The thickness distribution used for both the plane and the cambered wings is tabulated in table I and was a modified NACA 0003.9-65 section.

TESTS AND PROCEDURES

Range of Test Variables

Experimental data were obtained during the investigation over a Mach number range from 0.70 to 1.90 and over as wide a range of attitudes as was possible from structural considerations. In general, angles of attack from -4° to $+12^{\circ}$ were the limits of the range of this variable. Data were obtained for a Reynolds number of 3.0 million based on the wing mean aerodynamic chord.

At the low Reynolds numbers at which tests are conducted in most wind tunnels, the location of the transition from a laminar to a turbulent type of boundary layer is influenced by lift coefficient. In order that the comparisons made, particularly of the drag characteristics, be for a consistent type of boundary-layer flow throughout the lift-coefficient range, some means of maintaining transition at the same location for all lift coefficients is necessary. The results of reference 3 have indicated that turbulent flow on wings can be obtained by the use of wires. The wire size required to promote turbulent flow is dependent on test Mach number and the Reynolds number based on the mean aerodynamic chord.

[redacted]

On the basis of these results the data of the present investigation were obtained with 0.010-inch-diameter wire fixed on the body, vertical tail and on the wings near the leading edges (see fig. 3).

Reduction of Data

The data presented herein have been reduced to standard NACA coefficient form. The pitching-moment coefficients were referred to a lateral axis which passes through a point at $0.275\bar{c}$ behind the leading edge of the wing mean aerodynamic chord and $0.016\bar{c}$ above the mean aerodynamic chord. The drag coefficients were adjusted to take account of measured internal drag and are, therefore, external drag coefficients. Factors which affect the accuracy of the results are discussed in the following paragraphs.

Stream variations.- Extensive surveys of the stream characteristics were made in the Ames 6- by 6-foot wind tunnel throughout the available Mach number range. The data showed that over the model length essentially no stream curvature existed in the pitch plane of the model and that the axial static-pressure variations were less than ±1 percent of the dynamic pressure. For the models investigated herein this static-pressure variation resulted in negligible corrections to the drag due to longitudinal buoyancy. Therefore, no corrections to the data for stream curvature or static-pressure variations were made for the present investigation.

A stream angle was found to exist in the vertical plane in the test section (the pitch plane of the model) which varied with Mach number. Test of the model of the present investigation in both normal and inverted attitudes corroborated closely the magnitude of the stream angle obtained from a cone survey. The data presented herein have been adjusted for the stream angle which was as much as 0.25° downflow at a Mach number of 1.0.

Support interference.- The effects of model support interference on the aerodynamic characteristics were considered to consist primarily of a change in the base pressure of the model. The base pressure was measured, therefore, and the drag data were adjusted to correspond to a base pressure equal to the free-stream static pressure.

Tunnel wall interference.- In order to establish the usefulness of the 6- by 6-foot wind tunnel as a test facility, particularly at transonic and low supersonic speeds where reflected disturbances might affect the results, the tunnel calibration tests were extended to include models of various sizes and plan forms. These unpublished data indicate that as a result of the perforated floor and ceiling, reliable data could be obtained throughout the Mach number range of the facility with certain restrictions on model size and model attitude. Although the model geometric characteristics and range of model attitudes necessary to obtain

interference-free data have not been completely defined, sufficient data are available to indicate that for the configuration of the present investigation, the data obtained at transonic and low supersonic speeds are sufficiently free of wall interference effects that conclusions drawn would not be affected. Thus, no correction for this effect has been made.

RESULTS AND DISCUSSION

The complete results of this investigation are tabulated in table II. The portion of the data which are analyzed are also presented graphically. In figure 4(a) the drag results obtained for wings cambered over the outboard 10 percent of the local semispan for design lift coefficients of 0.10 and 0.20 are compared with those obtained for a plane wing. Figure 4(b) shows a similar comparison for wings cambered over the outboard 15 percent of the local semispan for design lift coefficients of 0.10, 0.20, and 0.30. Figures 5 through 8 are devoted to further comparisons of the drag results obtained from the plane and cambered wings. Lift and moment data are presented in figures 9, 10, and 11.

Drag Characteristics

The effectiveness of the various cambers in reducing the drag resulting from lift for the model of the present investigation can be seen in figure 4. A reduction of the drag resulting from lift is shown to exist throughout the test Mach number range for all the cambered wings, although a drag penalty was incurred near zero lift for the model having wings cambered for design lift coefficients of 0.20 and 0.30. The model with the wing cambered for a lift coefficient of 0.10, however, exhibited equal or less zero-lift drag than with the plane wing at Mach numbers less than 1.9. When the reasons for the reduction of drag at zero lift are considered, it is necessary to realize that for both the cambered and the plane wings zero wing lift (where drag due to wing lift was zero) occurred at some negative model lift coefficient (see fig. 10) as a result of the cambered body and wing-body interference effects. Therefore, at conditions of zero total lift a finite amount of positive lift was carried by the wings and the possibility of a reduction in drag for the cambered wings from that of the plane wing existed due to the development of an effective leading-edge thrust for the cambered wing.

To demonstrate more clearly the reduction in drag resulting from the effective leading-edge thrust developed by the cambered wings, a comparison is shown in figure 5 of the variation of drag coefficient with Mach number for the plane and cambered wings at several lift coefficients. A comparison of the results obtained for the wings cambered for a lift coefficient of 0.10 with those for the plane wing shows that significant

[redacted]

reductions in drag at lifting conditions were realized by the cambered wings at subsonic and transonic speeds with essentially no penalty in zero-lift drag. In the same speed range the wings incorporating greater amounts of camber realized even larger drag reductions for lift coefficients above 0.20 but at the expense of an increased drag at zero lift. Although the beneficial effects of the cambered leading edges were greatest at subsonic and transonic speeds, it appears that a portion of the effective leading-edge thrust was also realized at low supersonic speeds. At the higher supersonic speeds, however, the benefits of camber are considerably reduced and are restricted to lift coefficients of 0.30 and above. The unusual variation of the drag coefficient in the transonic speed range noted in figure 5(a) for the wing cambered for a lift coefficient of 0.10 is not consistent with the results of the other wings and is not clearly understood.

The preceding results have shown that large reductions in drag coefficients can be realized at subsonic and transonic speeds on a triangular wing with various amounts and extents of conical camber. The results shown in figure 6, which presents the incremental drag coefficients due to camber as a function of design lift coefficient at several Mach numbers, are included as a guide to indicate the amount of camber necessary to achieve the most desirable overall drag characteristics.

Examination of the results shown in figure 6 indicates that some amount of camber (or design lift coefficient) can usually be chosen beyond which further reductions of drag will not be realized for the usual cruise lift-coefficient range. It must be remembered, however, that the test lift coefficients shown in this figure are not those of the wing but those of the complete model and, hence, the drag increments shown are strictly applicable only for this particular model. It is evident from these data that for flight lift coefficients up to 0.20 the camber employed should not exceed that corresponding to the design lift coefficient of about 0.20. For flight lift coefficients above 0.20 the results of figure 6(b) show that greater amounts of camber resulted in large reductions in drag at subsonic speeds. However, such increases in amount of camber were accompanied by increases in the zero-lift drag throughout the speed range.

The effects of the spanwise extent of the camber on the drag characteristics may be seen by comparison of figure 6(b) with figure 6(a). For design lift coefficients of 0.10 there was little difference in the results obtained for the wings cambered over 10 and 15 percent of the local semispan. For design lift coefficients of 0.20, however, the data indicate that the wing cambered over the 15-percent semispan had somewhat superior drag characteristics than did the wing cambered over 10 percent of the semispan. This is apparently due to the smaller penalty in drag at zero lift that is associated with the more gradual contouring of the wing cambered over 15 percent of the semispan.

[redacted]

To permit assessment of the effects of conical camber on the lift-drag characteristics of the model, figure 7 presents a comparison of lift-drag ratio as a function of lift coefficient for the model with the plane and cambered wings. The beneficial effect of the camber is again evident for Mach numbers up through 1.2 and, furthermore, it is shown that this effect exists for all test lift coefficients above about 0.10.

In figure 8, the maximum lift-drag ratios measured for the plane-wing model and the models with the various cambered leading edges are summarized as functions of Mach number. For comparative purposes, curves are also shown corresponding to the full and no leading-edge suction cases for a wing of this plan form calculated from the values of zero-lift drag measured for the model with the plane wing. Inasmuch as these experimental zero-lift drags do not correspond to conditions of zero wing lift these curves are not strictly applicable to the test wing-body-tail combinations. They present, however, an approximate means of comparing the proportions of the available leading-edge thrusts obtained by the cambered wings.

If the calculated curves are assumed to be limits of the effect of leading-edge suction, the most highly cambered wing ($C_{L_d} = 0.30$) can be seen to have attained a value of maximum lift-drag ratio approaching that for full leading-edge thrust at a Mach number of 0.70 (see fig. 8(b)). Although somewhat lower than for the wing cambered for a lift coefficient of 0.30, the maximum lift-drag ratios for the wings cambered for design lift coefficients of 0.10 and 0.20 were equal to or higher than those for the plane wing for Mach numbers up to 1.5. Even for a Mach number of 1.9 only the wing cambered over the outboard 10 percent of the local semispan for a lift coefficient of 0.20 experienced a measurable reduction of maximum lift-drag ratio below that for the plane wing. In general, increasing the extent of the camber from 10- to 15-percent semispan resulted in only slight changes in the maximum lift-drag ratio. As a point of general interest it should be mentioned that the unusual variation of maximum lift-drag ratio at transonic speeds for the wing cambered for a lift coefficient of 0.10 shown in figure 8(a) is not clearly understood. It results, however, from the aforementioned decrease in drag at lift shown for this configuration in this speed range (see fig. 5(a)).

In order to show the effects of camber on the lift coefficient for maximum lift-drag ratio, figure 9 is included which presents $C_{L_{opt}}$ as a function of Mach number. The results are of interest in that they show that the cambered wings realize the maximum lift-drag ratio at lift coefficients which are not greatly different from that of the plane wing.

[redacted]

Lift and Moment Characteristics

During this investigation experimental results were also obtained showing the effects of conical camber on the lift and moment characteristics of the test models. The lift and pitching-moment curves shown in figures 10 and 11 for the cambered wings are essentially parallel with those for the plane wing and displaced only slightly. A small positive shift in the angle for zero lift which is due to effective washout resulting from camber is of little significance but the positive shift in pitching moment should result in a small decrease in trim drag.

CONCLUSIONS

An experimental investigation was made to determine the effectiveness of various amounts and extents of conical camber in reducing the drag resulting from lift on a triangular wing of aspect ratio 2.2 in combination with a body and vertical tail. The results of this investigation showed:

1. The use of a moderate amount of conical camber resulted in significant drag reductions throughout the range of positive lift coefficients for subsonic and transonic speeds. Furthermore, some reduction of drag at lifting conditions was achieved at supersonic speeds with essentially no penalty in drag at zero lift.

2. The use of greater amounts of camber produced large reductions of drag at high lift coefficients for subsonic and transonic speeds with little penalty in drag at zero lift. The camber was effective in reducing the drag at high supersonic speeds only at lift coefficients of 0.30 and above.

3. Changing the extent of the cambered area from 10 percent to 15 percent of the local semispan resulted in slight improvements in drag characteristics for a design lift coefficient of 0.20.

4. The lift and pitching-moment characteristics were not significantly affected by the camber.

Ames Aeronautical Laboratory
National Advisory Committee for Aeronautics
Moffett Field, Calif., Jan. 10, 1957

[redacted]

REFERENCES

1. Hall, Charles F.: Lift, Drag and Pitching Moment of Low-Aspect-Ratio Wings at Subsonic and Supersonic Speeds. NACA RM A53A30, 1953.

2. Boyd, John W., Migotsky, Eugene, and Wetzel, Benton E.: A Study of Conical Camber for Triangular and Sweptback Wings. NACA RM A55G19, 1955.

3. Winter, K. G., Scott-Wilson, J. B., and Davies, F. V.: Methods of Determination and of Fixing Boundary-Layer Transition on Wind Tunnel Models at Supersonic Speeds. R.A.E. TN Aero. 2341, British, Sept. 1954.

[redacted]

TABLE I.- THICKNESS DISTRIBUTION OF WINGS

x/c	z/c
0	0
.0050	±.0038
.0100	±.0052
.0250	±.0077
.0500	±.0100
.1000	±.0128
.2000	±.0159
.3000	±.0178
.4000	±.0188
.5000	±.0194
.6000	±.0192
.7000	±.0177
.8000	±.0136
.9000	±.0070
1.0000	0
L.E.R. = 0.0017c	

TABLE II.- AERODYNAMIC COEFFICIENTS FOR MODEL HAVING A TRIANGULAR WING OF ASPECT RATIO 2.2, 3.9 PERCENT THICK; R = 3.0×10^6

(a) Uncambered Wing

M	α, deg	C_L	C_D	C_m	M	α, deg	C_L	C_D	C_m
0.70	-4.32	-0.229	0.0261	0.024	1.00	-4.90	-0.308	0.0454	0.061
	-2.07	-.122	.0154	.014		-2.55	-.171	.0270	.037
	-.96	-.072	.0132	.008		-1.45	-.113	.0235	.027
	.14	-.023	.0123	.004		-.29	-.053	.0208	.018
	1.20	.026	.0125	-.000		.81	.003	.0203	.009
	2.34	.081	.0139	-.006		1.97	.063	.0203	.001
	3.53	.138	.0173	-.011		3.21	.136	.0244	-.011
	4.61	.192	.0233	-.016		4.35	.206	.0320	-.022
	6.73	.311	.0421	-.026		6.56	.349	.0528	-.044
	9.04	.435	.0717	-.034		9.01	.507	.0943	-.077
0.90	-4.61	-.274	.0321	.038	1.20	-4.81	-.281	.0486	.069
	-2.32	-.153	.0180	.024		-2.45	-.151	.0325	.042
	-1.23	-.097	.0146	.016		-1.35	-.094	.0283	.030
	-.03	-.041	.0130	.009		-.19	-.032	.0258	.018
	1.04	.012	.0130	.003		.90	.023	.0254	.007
	2.21	.070	.0144	-.004		2.08	.085	.0271	-.006
	3.43	.134	.0183	-.012		3.32	.155	.0318	-.020
	4.51	.195	.0247	-.018		4.45	.219	.0389	-.033
	6.80	.330	.0470	-.034		6.70	.348	.0608	-.059
	9.20	.473	.0826	-.051		9.03	.475	.0934	-.085
0.95	-4.82	-.300	.0371	.054	1.50	-4.43	-.213	.0408	.051
	-2.47	-.170	.0204	.033		-2.12	-.110	.0283	.029
	-1.36	-.112	.0165	.024		-1.03	-.062	.0253	.019
	-.20	-.052	.0142	.015		.11	-.010	.0240	.009
	.89	.007	.0137	.006		1.20	.038	.0243	-.001
	2.04	.067	.0147	-.003		2.30	.090	.0265	-.011
	3.29	.136	.0189	-.013		3.58	.149	.0314	-.024
	4.42	.203	.0261	-.022		4.68	.200	.0378	-.035
	6.65	.342	.0488	-.041		6.87	.300	.0562	-.055
	9.12	.498	.0872	-.066		9.17	.398	.0829	-.076

M	α, deg	C_L	C_D	C_m
1.90	-4.56	-0.170	0.0366	0.034
	-2.31	-.091	.0260	.019
	-1.21	-.053	.0231	.011
	-.04	-.010	.0218	.003
	.94	.025	.0217	-.004
	2.09	.064	.0234	-.012
	3.27	.108	.0267	-.021
	4.32	.144	.0312	-.028
	6.41	.219	.0438	-.043
	8.65	.293	.0628	-.058

[redacted]

TABLE II.- AERODYNAMIC COEFFICIENTS FOR MODEL HAVING A TRIANGULAR WING OF ASPECT RATIO 2.2, 3.9 PERCENT THICK; R = 3.0×10^6 - Continued

(b) Wing cambered over outboard 10 percent of local semispan, $C_{L_d} = 0.10$ at M = 1.0

M	α, deg	C_L	C_D	C_m	M	α, deg	C_L	C_D	C_m
0.70	-4.31	-0.251	0.0316	0.027	1.00	-4.95	-0.331	0.0519	0.067
	-2.05	-.139	.0187	.017		-2.65	-.194	.0317	.043
	-.98	-.086	.0153	.012		-1.48	-.131	.0251	.032
	.14	-.034	.0132	.007		-.31	-.067	.0221	.029
	1.14	.016	.0125	.002		.78	-.008	.0193	.012
	2.26	.066	.0128	-.002		1.94	.052	.0185	.003
	3.44	.120	.0148	-.007		3.11	.113	.0198	-.006
	4.56	.174	.0177	-.012		4.29	.180	.0245	-.014
	6.66	.278	.0298	-.021		6.53	.331	.0454	-.041
	8.97	.409	.0610	-.031		8.95	.484	.0838	-.071
	13.52	.634	.1449	-.045		11.30	.629	.1326	-.099
0.90	-4.64	-.301	.0385	.045	1.20	-4.91	.300	.0544	.074
	-2.32	-.173	.0214	.028		-2.55	-.168	.0353	.047
	-1.24	-.116	.0168	.021		-1.37	-.106	.0296	.034
	-.05	-.053	.0137	.013		-.20	-.043	.0264	.021
	1.03	.002	.0129	.006		.85	.014	.0250	.009
	2.18	.057	.0132	-.000		2.01	.074	.0257	-.003
	3.33	.115	.0160	-.008		3.25	.140	.0285	-.016
	4.49	.174	.0194	-.014		4.41	.206	.0342	-.030
	6.66	.297	.0368	-.027		6.64	.335	.0531	-.056
	9.06	.443	.0723	-.044		9.06	.466	.0858	-.082
	10.28	.515	.0944	-.052		13.69	.699	.1745	-.132
0.95	-4.83	-.321	.0421	.058	1.50	-4.51	-.224	.0444	.054
	-2.49	-.190	.0233	.038		-2.15	-.120	.0300	.032
	-1.44	-.130	.0183	.031		-1.06	-.071	.0262	.022
	-.22	-.064	.0145	.019		.09	-.019	.0241	.011
	.87	-.005	.0126	.009		1.19	.031	.0240	.001
	2.02	.053	.0127	.001		2.34	.083	.0256	-.009
	3.13	.114	.0146	-.008		3.50	.136	.0292	-.020
	4.31	.176	.0179	-.016		4.64	.188	.0348	-.031
	6.55	.311	.0372	-.033		6.85	.289	.0517	-.053
	8.95	.469	.0744	-.059		9.13	.387	.0765	-.073
	10.13	.540	.0959	-.067		13.61	.563	.1458	-.110

M	α, deg	C_L	C_D	C_m
1.90	-4.54	-0.180	0.0396	0.036
	-1.25	-.065	.0249	.014
	-2.30	-.103	.0281	.021
	-.11	-.024	.0229	.006
	.94	.013	.0226	-.002
	2.06	.053	.0234	-.009
	3.18	.094	.0261	-.018
	4.30	.133	.0300	-.026
	6.41	.207	.0414	-.041
	8.61	.283	.0591	-.056
	13.05	.418	.1093	-.083

[redacted]

TABLE II.- AERODYNAMIC COEFFICIENTS FOR MODEL HAVING A TRIANGULAR WING OF ASPECT RATIO 2.2, 3.9 PERCENT THICK; R = 3.0×10^6 - Continued

(c) Wing cambered over outboard 10 percent of local semispan, $C_{L_d} = 0.20$ at M = 1.0

M	α, deg	C_L	C_D	C_m	M	α, deg	C_L	C_D	C_m
0.70	-4.47	-0.276	0.0398	0.030	1.00	-5.02	-0.352	0.0617	0.072
	-2.09	-.155	.0235	.019		-2.69	-.214	.0357	.047
	-1.02	-.103	.0191	.014		-1.52	-.149	.0308	.037
	.11	-.047	.0161	.009		-.35	-.085	.0255	.026
	1.17	.003	.0145	.004		.76	-.022	.0224	.016
	2.24	.054	.0144	0		1.92	.040	.0219	.007
	3.48	.113	.0155	-.006		3.10	.106	.0223	-.003
	4.49	.162	.0175	-.011		4.21	.168	.0247	-.012
	6.63	.263	.0256	-.019		6.47	.307	.0380	-.034
	8.90	.380	.0451	-.029		8.93	.470	.0739	-.067
						11.25	.614	.1203	-.092
0.90	-4.74	-.323	.0508	.049	1.20	-4.88	.312	.0603	.078
	-2.37	-.193	.0272	.032		-2.52	-.181	.0395	.050
	-1.24	-.132	.0212	.024		-1.42	-.123	.0336	.039
	-.09	-.072	.0173	.017		-.29	-.060	.0292	.026
	.95	-.015	.0153	.009		.87	.001	.0272	.013
	2.16	.045	.0149	.002		1.99	.063	.0272	0
	3.37	.107	.0160	-.006		3.22	.131	.0298	-.014
	4.45	.163	.0186	-.012		4.38	.194	.0345	-.027
	6.63	.279	.0299	-.024		6.59	.319	.0506	-.051
	9.04	.415	.0581	-.039		9.00	.450	.0787	-.078
						13.63	.687	.1650	-.128
0.95	-4.94	-.351	.0520	-.067	1.50	-4.49	-.234	.0493	.056
	-2.58	-.213	.0301	.045		-2.24	-.134	.0341	.035
	-1.44	-.149	.0232	.034		-1.09	-.084	.0295	.025
	-.26	-.084	.0184	.023		.05	-.032	.0267	.015
	.84	-.022	.0162	.013		1.16	.020	.0261	.004
	3.22	.108	.0178	-.006		2.32	.071	.0272	-.006
	2.00	.043	.0156	.003		3.48	.126	.0305	-.018
	4.33	.168	.0199	-.015		4.63	.178	.0358	-.029
	6.51	.292	.0333	-.030		6.83	.276	.0508	-.049
	8.89	.430	.0624	-.044		9.14	.377	.0743	-.070

M	α, deg	C_L	C_D	C_m
1.90	-4.61	-0.186	0.0437	0.037
	-2.32	-.110	.0316	.023
	-1.25	-.073	.0277	.016
	-.19	-.034	.0255	.008
	.87	.003	.0248	.001
	2.02	.042	.0253	-.006
	3.13	.083	.0276	-.015
	4.28	.122	.0311	-.022
	6.35	.195	.0414	-.037
	8.59	.271	.0578	-.053

[redacted]

TABLE II.- AERODYNAMIC COEFFICIENTS FOR MODEL HAVING A TRIANGULAR WING OF ASPECT RATIO 2.2, 3.9 PERCENT THICK; R = 3.0×10^6 - Continued

(d) Wing cambered over outboard 15 percent of local semispan, $C_{L_d} = 0.10$ at M = 1.0

M	α, deg	C_L	C_D	C_m	M	α, deg	C_L	C_D	C_m
0.70	-4.36	-0.248	0.0321	0.025	1.00	-4.97	-0.329	0.0512	0.066
	-2.10	-.134	.0185	.016		-2.58	-.190	.0293	.041
	-1.03	-.084	.0151	.011		-1.53	-.129	.0252	.031
	.14	-.030	.0129	.006		-.31	-.064	.0210	.020
	1.19	.018	.0125	.001		.78	-.006	.0183	.011
	2.27	.064	.0130	-.002		1.94	.053	.0182	.002
	3.43	.118	.0148	-.007		3.10	.111	.0203	-.005
	4.54	.169	.0179	-.012		4.28	.178	.0243	-.014
	6.67	.282	.0323	-.022		6.50	.324	.0434	-.038
	9.02	.411	.0616	-.031		8.95	.484	.0821	-.070
	10.16	.462	.0783	-.031		11.30	.627	.1309	-.097
0.90	-4.69	-.299	.0399	.043	1.20	-4.87	-.298	.0540	.073
	-2.30	-.167	.0220	.026		-2.49	-.166	.0350	.046
	-1.20	-.111	.0173	.020		-1.43	-.107	.0298	.034
	-.04	-.051	.0146	.012		-.26	-.045	.0265	.021
	1.04	.003	.0138	.005		.84	.012	.0251	.010
	2.18	.056	.0142	-.001		2.07	.075	.0260	-.003
	3.33	.113	.0161	-.007		3.25	.140	.0286	-.016
	4.49	.173	.0200	-.014		4.43	.207	.0341	-.030
	6.72	.300	.0383	-.028		6.69	.337	.0538	-.056
	9.09	.443	.0720	-.044		9.00	.463	.0853	-.081
						13.79	.756	.1861	-.150
0.95	-4.83	-.321	.0430	.057	1.50	-4.56	-.228	.0450	.054
	-2.54	-.189	.0242	.038		-2.17	-.120	.0302	.032
	-1.38	-.125	.0184	.028		-1.12	-.074	.0265	.022
	-.22	-.061	.0146	.017		.04	-.021	.0242	.012
	2.02	.053	.0137	0		1.14	.030	.0239	.002
	3.13	.113	.0152	-.009		2.35	.083	.0254	-.009
	4.35	.178	.0196	-.017		3.48	.137	.0291	-.021
	6.56	.314	.0390	-.035		4.68	.190	.0349	-.032
	9.01	.465	.0746	-.056		6.86	.291	.0519	-.053
	10.15	.537	.0968	-.067		9.15	.391	.0775	-.074
						13.70	.570	.1486	-.111

M	α, deg	C_L	C_D	C_m
1.90	-4.60	-0.183	0.0399	0.036
	-2.31	-.105	.0281	.022
	-1.26	-.068	.0246	.015
	-.17	-.028	.0225	.007
	.89	.011	.0221	-.001
	2.00	.049	.0231	-.008
	3.18	.091	.0257	-.016
	4.30	.131	.0295	-.025
	6.43	.206	.0411	-.040
	8.66	.282	.0591	-.056
	13.02	.422	.1101	-.084

[redacted]

TABLE II.- AERODYNAMIC COEFFICIENTS FOR MODEL HAVING A TRIANGULAR WING OF ASPECT RATIO 2.2, 3.9 PERCENT THICK; R = 3.0×10^6 - Continued

(e) Wing cambered over outboard 15 percent of local semispan, $C_{L_d} = 0.20$ at M = 1.0

M	α, deg	C_L	C_D	C_m	M	α, deg	C_L	C_D	C_m
0.70	-4.41	-0.269	0.0390	0.028	1.00	-5.03	-0.349	0.0606	0.070
	-2.10	-.152	.0232	.017		-2.69	-.212	.0380	.046
	-1.05	-.098	.0187	.013		-1.51	-.147	.0300	.035
	.12	-.044	.0155	.008		-.34	-.081	.0245	.024
	1.18	.007	.0140	.003		.76	-.020	.0215	.014
	2.34	.056	.0138	-.001		1.92	.042	.0209	.005
	3.42	.113	.0153	-.007		3.08	.101	.0220	-.003
	4.54	.163	.0174	-.011		4.25	.167	.0239	-.012
	6.68	.264	.0257	-.020		6.51	.309	.0381	-.037
	8.90	.377	.0460	-.029		8.90	.467	.0739	-.068
	13.50	.621	.1349	-.044		11.23	.611	.1202	-.093
0.90	-4.69	-.323	.0479	.048	1.20	-4.94	-.315	.0606	.077
	-2.36	-.188	.0277	.029		-2.59	-.183	.0396	.050
	-1.24	-.128	.0218	.022		-1.42	-.122	.0332	.038
	-.08	-.067	.0180	.014		-.29	-.058	.0289	.024
	1.01	-.010	.0159	.007		.87	.004	.0267	.012
	2.16	.048	.0154	.001		1.99	.063	.0262	-.000
	3.31	.107	.0169	-.006		3.22	.127	.0286	-.013
	4.43	.164	.0195	-.013		4.35	.191	.0328	-.026
	6.68	.280	.0305	-.025		6.64	.320	.0494	-.052
	9.02	.422	.0618	-.040		8.99	.453	.0779	-.079
	10.24	.492	.0833	-.047		13.67	.689	.1653	-.128
0.95	-4.89	-.349	.0524	.066	1.50	-4.52	-.234	.0490	.056
	-2.59	-.207	.0294	.040		-2.19	-.134	.0336	.035
	-1.44	-.145	.0228	.030		-1.09	-.084	.0291	.025
	-.29	-.079	.0182	.021		.05	-.033	.0261	.015
	.84	-.018	.0155	.011		1.10	.018	.0252	.004
	1.95	.044	.0149	.002		2.26	.070	.0259	-.006
	3.12	.104	.0160	-.007		3.48	.125	.0293	-.018
	4.33	.168	.0192	-.016		4.57	.176	.0342	-.028
	6.50	.290	.0308	-.031		6.76	.274	.0491	-.049
	8.98	.446	.0659	-.053		9.08	.376	.0728	-.071
	10.15	.518	.0865	-.062		13.62	.560	.1407	-.110

M	α, deg	C_L	C_D	C_m
1.90	-4.61	-0.187	0.0435	0.037
	-2.36	-.111	.0313	.023
	-1.29	-.074	.0273	.016
	-.14	-.034	.0248	.008
	.92	.003	.0239	.001
	1.99	.042	.0245	-.007
	3.16	.084	.0268	-.015
	4.27	.124	.0301	-.023
	6.37	.199	.0408	-.038
	8.65	.275	.0577	-.053
	13.00	.415	.1059	-.082

[redacted]

TABLE II.- AERODYNAMIC COEFFICIENTS FOR MODEL HAVING A TRIANGULAR WING OF ASPECT RATIO 2.2, 3.9 PERCENT THICK; R = 3.0×10^6 - Concluded

(f) Wing cambered over outboard 15 percent of local semispan, $C_{L_d} = 0.30$ at M = 1.0

M	α, deg	C_L	C_D	C_m	M	α, deg	C_L	C_D	C_m
0.70	-4.40	-0.290	0.0440	0.032	1.00	-5.04	-0.370	0.0680	0.076
	-2.12	-.173	.0266	.021		-2.73	-.232	.0424	.051
	-1.10	-.119	.0215	.016		-1.58	-.169	.0336	.040
	.03	-.063	.0175	.011		-.42	-.103	.0279	.029
	1.15	-.008	.0149	.006		.71	-.040	.0235	.019
	2.28	.045	.0141	.002		1.89	.027	.0219	.010
	3.41	.103	.0142	-.004		3.06	.092	.0211	0
	4.52	.155	.0162	-.009		4.24	.157	.0229	-.009
	6.61	.255	.0228	-.017		6.44	.294	.0351	-.031
	8.92	.364	.0365	-.026		8.82	.446	.0625	-.061
	11.18	.496	.0741	-.038		11.26	.600	.1112	-.090
0.90	-4.74	-.349	.0548	.055	1.20	-4.91	-.329	.0652	.081
	-2.45	-.213	.0324	.035		-2.56	-.200	.0427	.055
	-1.34	-.151	.0254	.027		-1.50	-.139	.0358	.042
	-.14	-.088	.0202	.019		-.28	-.076	.0304	.029
	.97	-.028	.0173	.012		.84	-.013	.0275	.016
	2.13	.033	.0162	.004		2.01	.050	.0265	.003
	3.30	.096	.0165	-.003		3.15	.116	.0276	-.010
	4.46	.156	.0185	-.010		4.37	.183	.0318	-.023
	6.66	.271	.0275	-.023		6.56	.306	.0469	-.048
	8.99	.396	.0469	-.034		8.91	.436	.0731	-.074
	11.41	.553	.0984	-.055		13.60	.678	.1557	-.126
0.95	-4.97	-.371	.0628	.071	1.50	-4.54	-.247	.0527	.059
	-2.58	-.231	.0345	.048		-2.25	-.145	.0363	.038
	-1.49	-.169	.0270	.038		-1.12	-.096	.0309	.028
	-.30	-.100	.0206	.026		.03	-.044	.0272	.017
	.75	-.037	.0169	.016		1.13	.006	.0258	.008
	1.97	.028	.0156	.007		2.28	.057	.0262	-.002
	3.09	.092	.0155	-.003		3.45	.114	.0291	-.015
	4.31	.158	.0182	-.012		4.61	.168	.0337	-.026
	6.54	.279	.0286	-.027		6.80	.267	.0481	-.047
	8.91	.414	.0539	-.041		9.11	.367	.0704	-.067
	11.32	.575	.1016	-.070		13.59	.552	.1347	-.107
1.90	-4.59	-0.192	0.0460	0.038					
	-2.40	-.117	.0332	.024					
	-1.32	-.081	.0290	.017					
	-.16	-.041	.0259	.009					
	.86	-.005	.0247	.002					
	2.02	.034	.0247	-.005					
	3.14	.074	.0267	-.013					
	4.25	.113	.0297	-.021					
	6.35	.191	.0398	-.037					
	8.65	.268	.0561	-.052					
	13.01	.408	.1023	-.080					

[redacted]

[redacted]

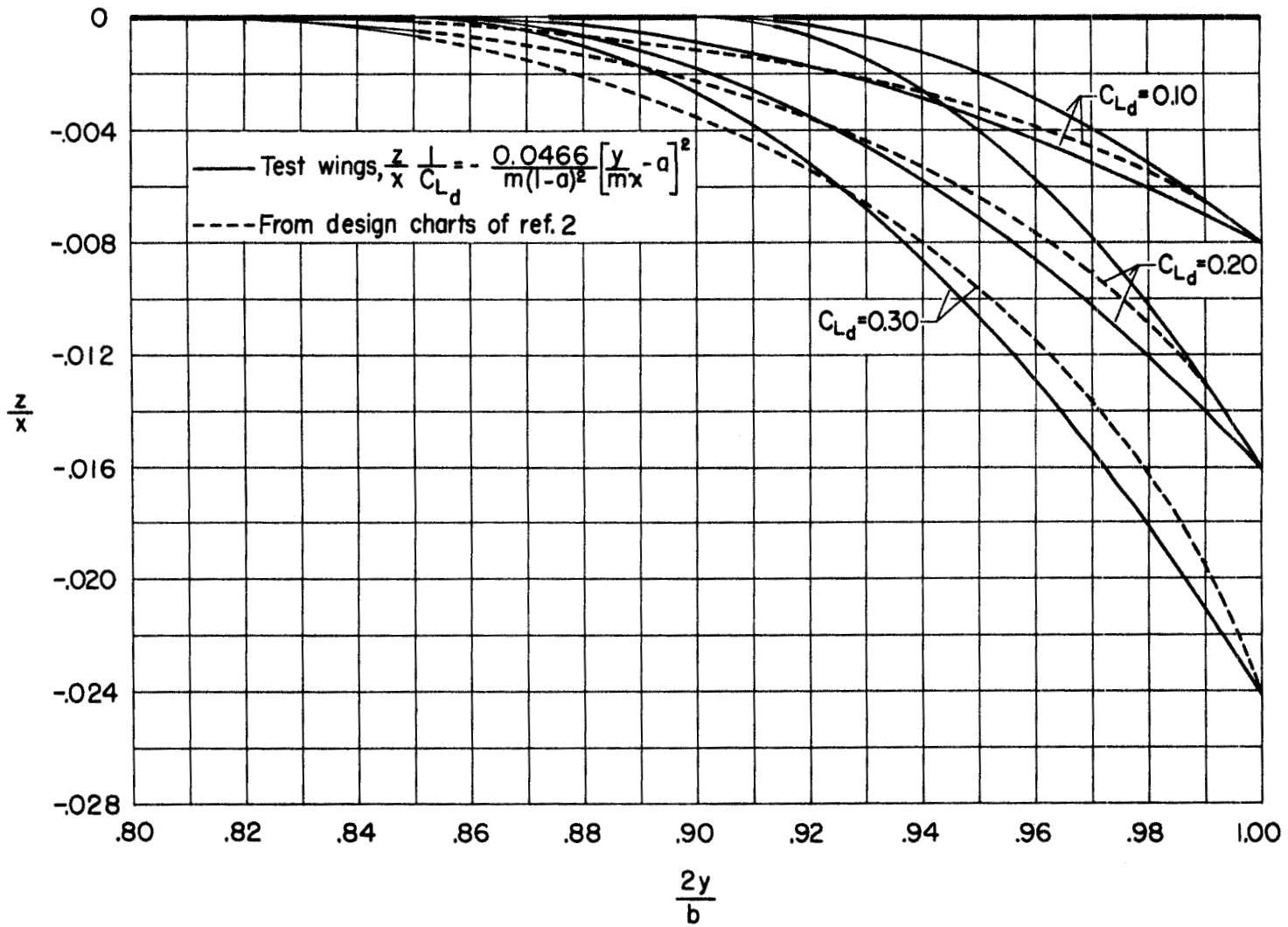

Figure 1.- Ordinates of the cambered surfaces.

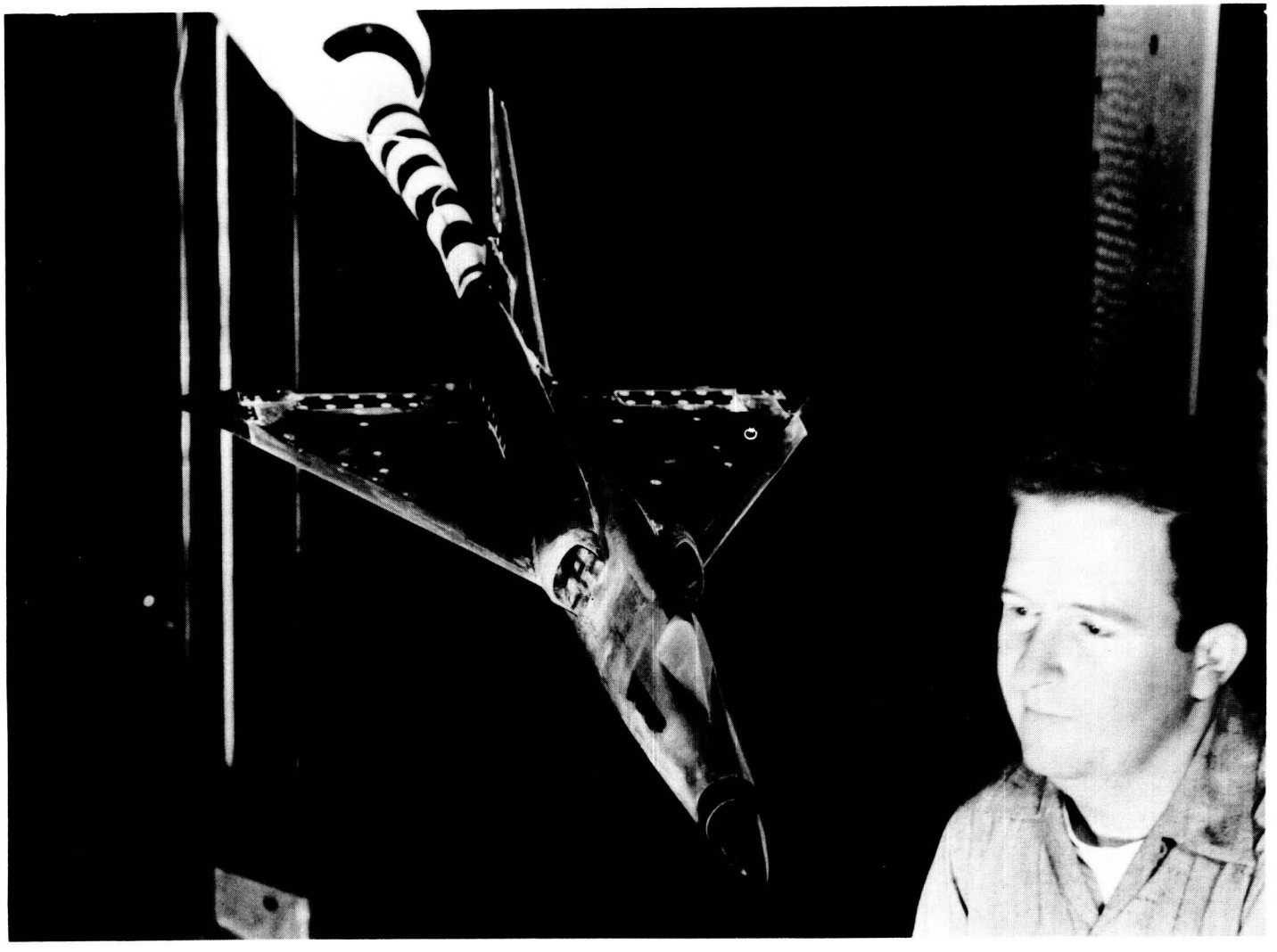

A-20980.1

Figure 2.- Model mounted in the 6- by 6-foot wind tunnel.

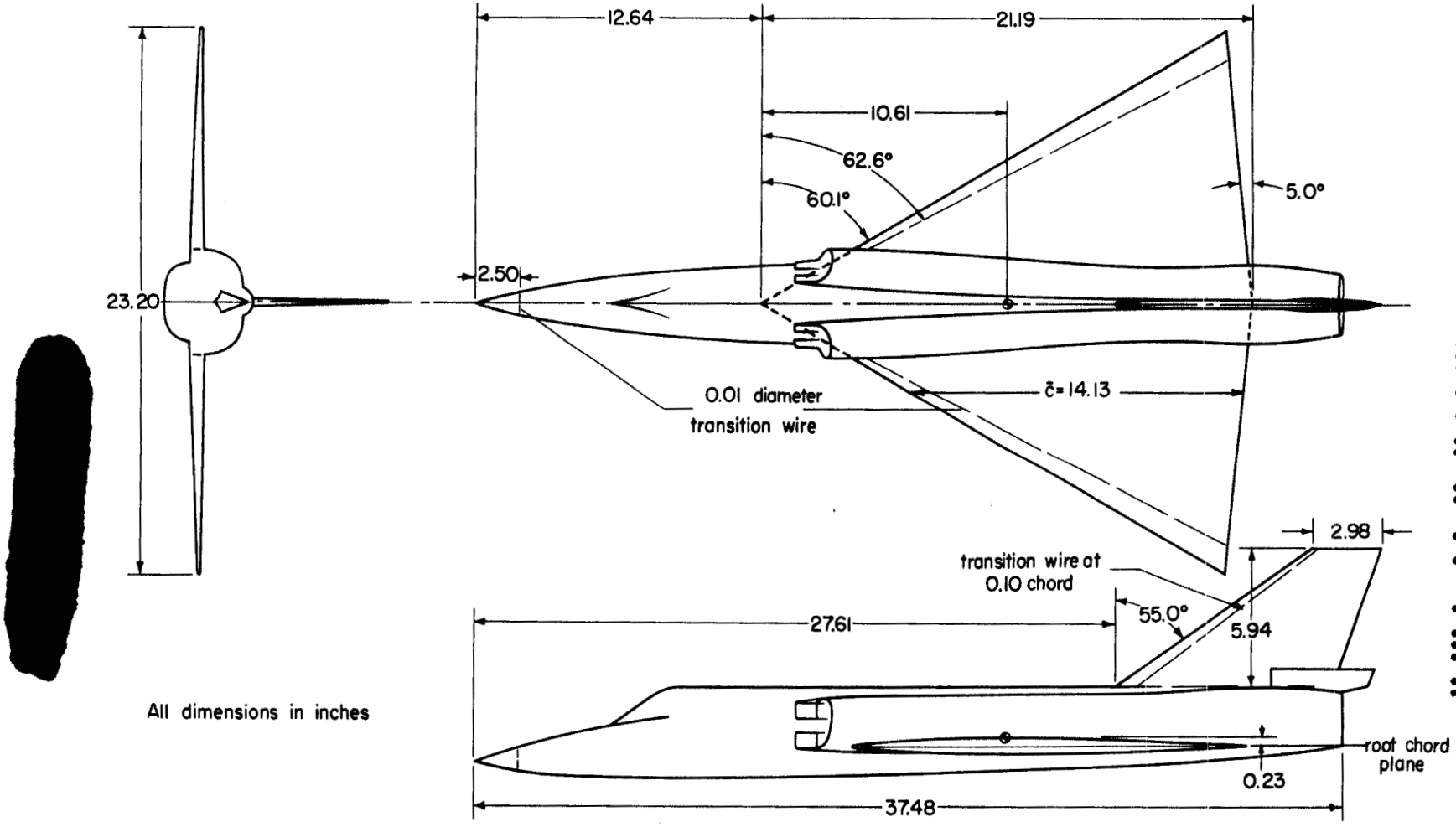

Figure 3.- Dimensional sketch of model.

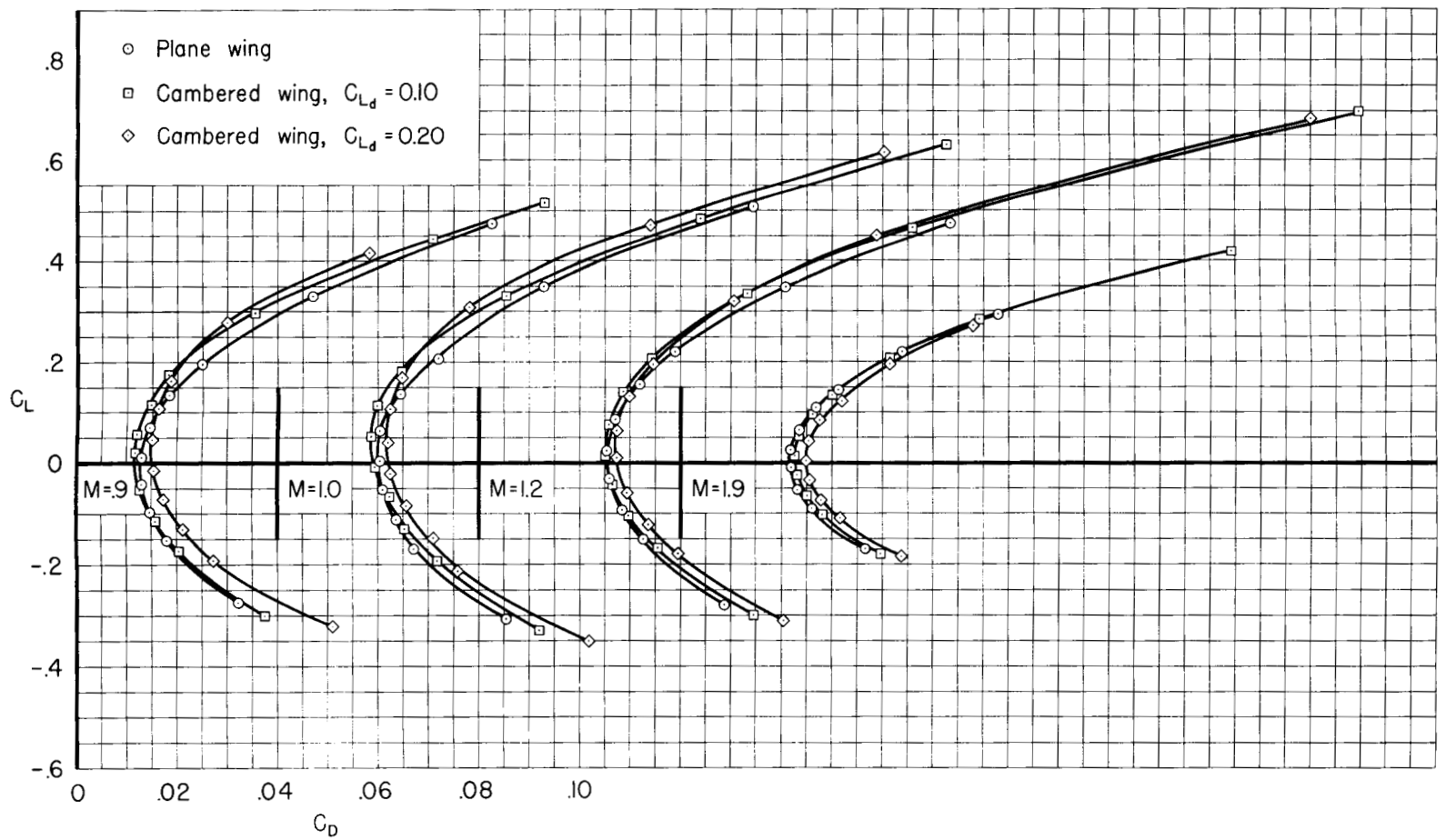

(a) Cambered over 10 percent of local semispan.

Figure 4.- Effect of conical camber on the variation of drag coefficient with lift coefficient.

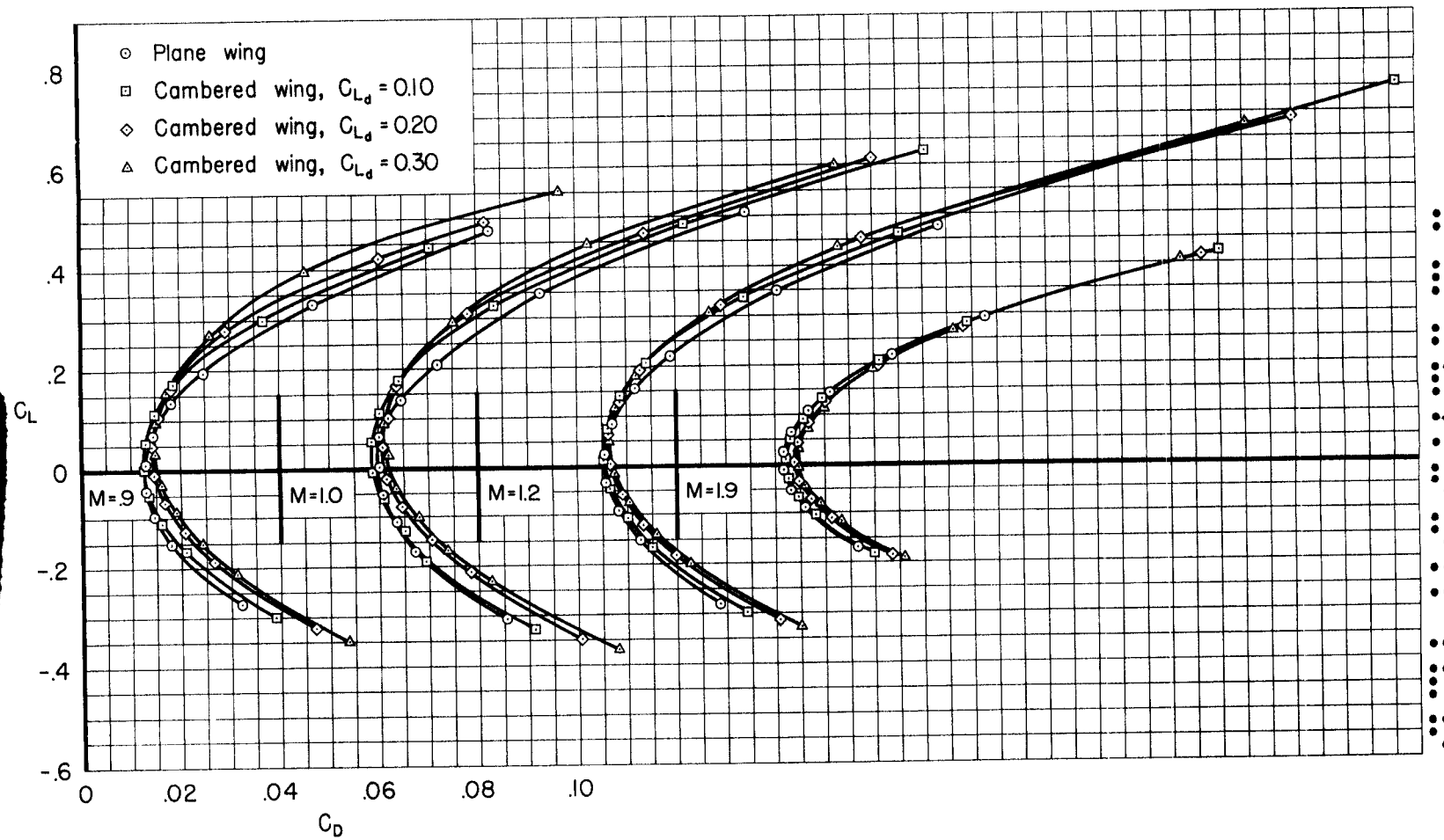

(b) Cambered over 15 percent of local semispan.

Figure 4.- Concluded.

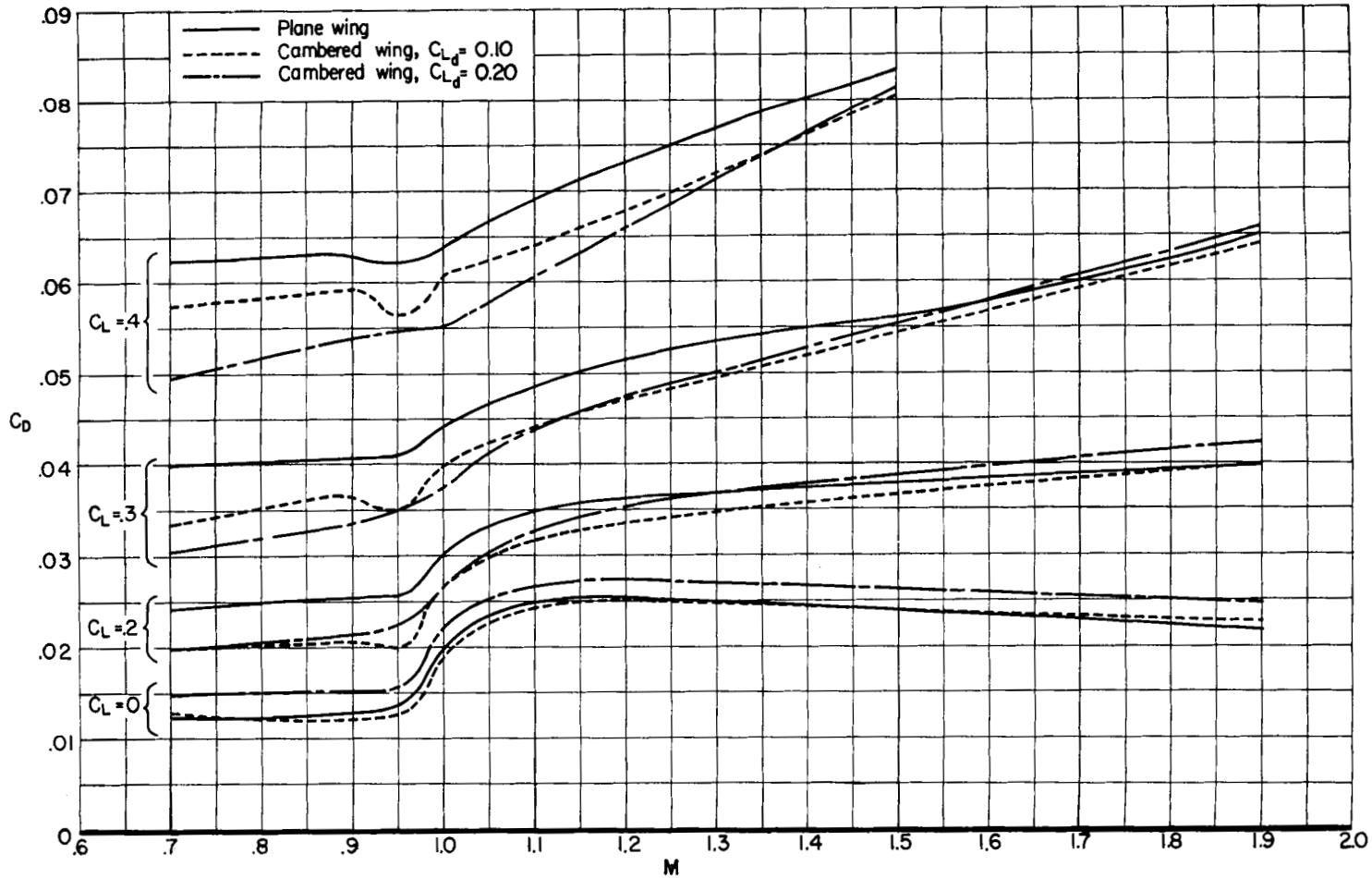

(a) Cambered over 10 percent of local semispan.

Figure 5.- Effect of conical camber on the variation of drag coefficient with Mach number for several lift coefficients.

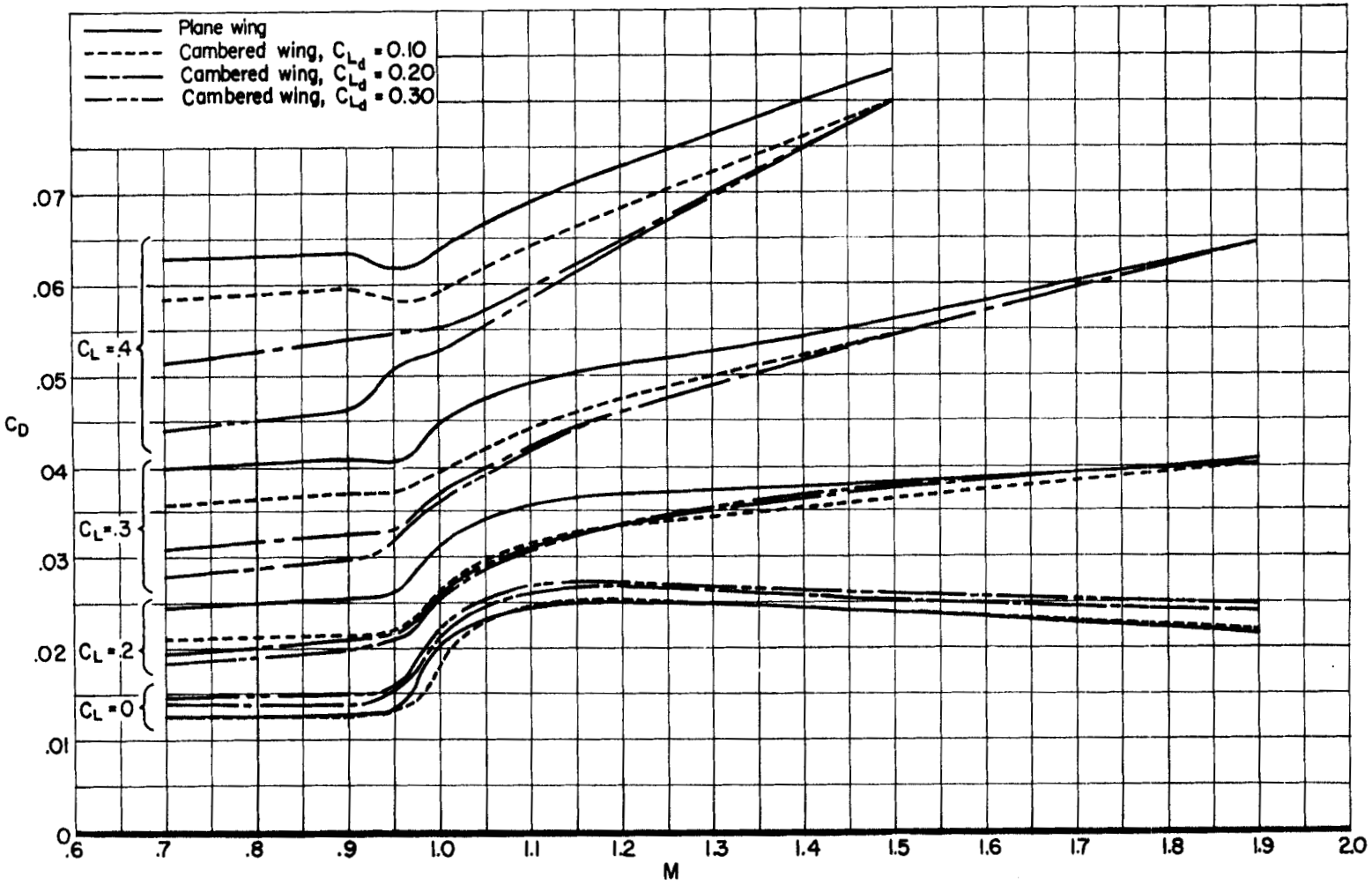

(b) Cambered over 15 percent of local semispan.

Figure 5.- Concluded.

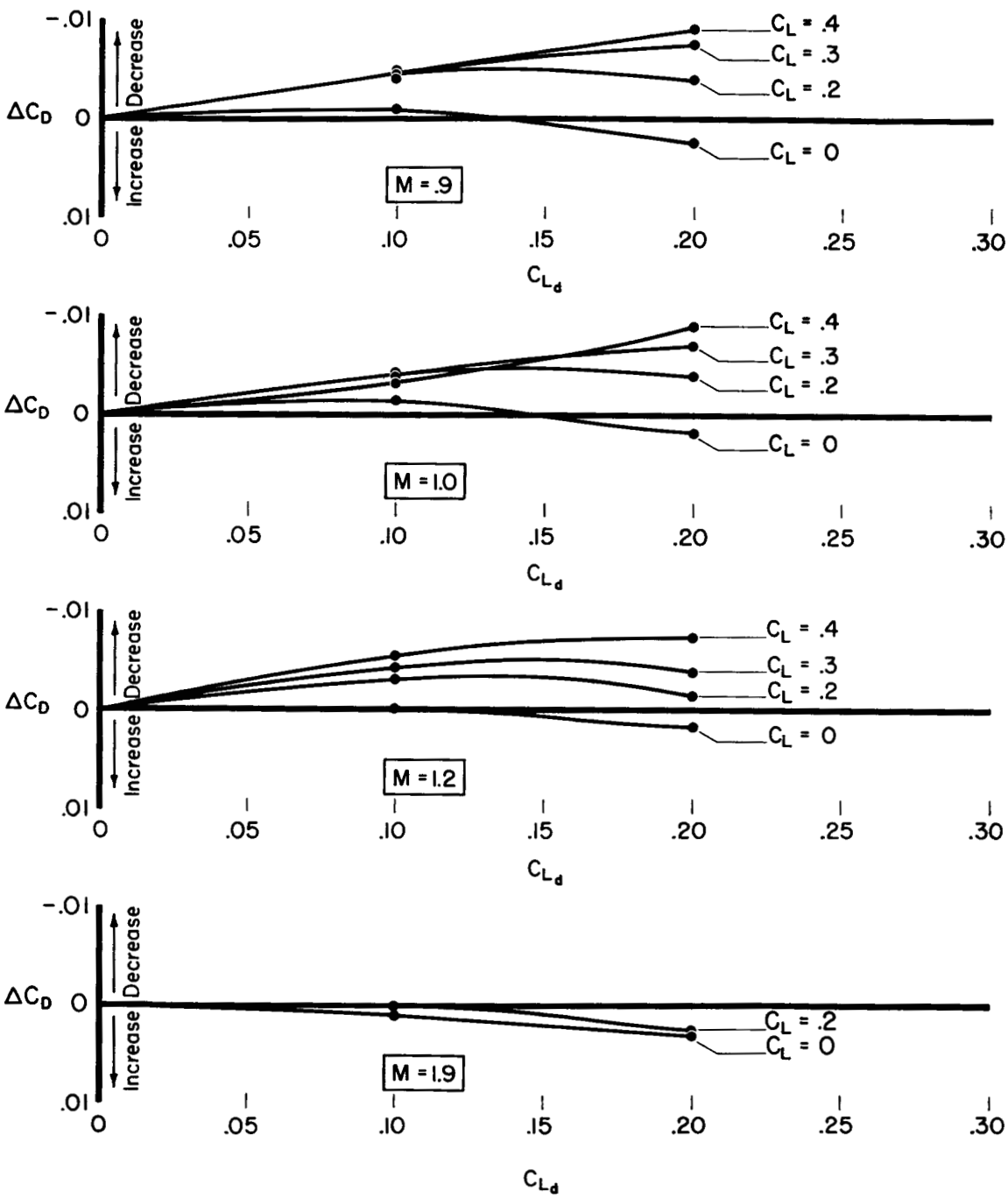

(a) Cambered over 10 percent of the local semispan.

Figure 6.- Variation of incremental drag coefficient due to camber with design lift coefficient for several lift coefficients.

[redacted]

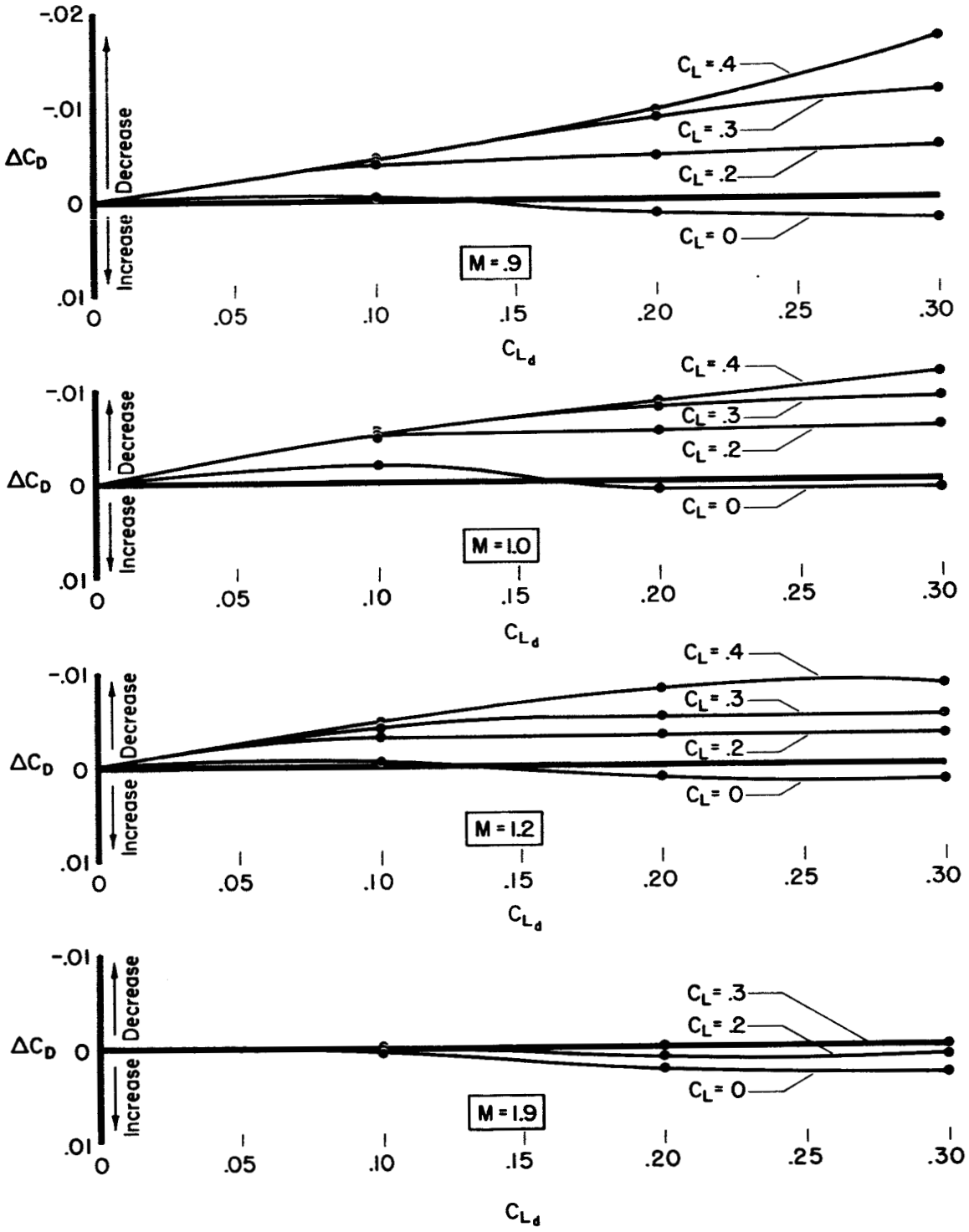

(b) Cambered over 15 percent of the local semispan.

Figure 6.- Concluded.

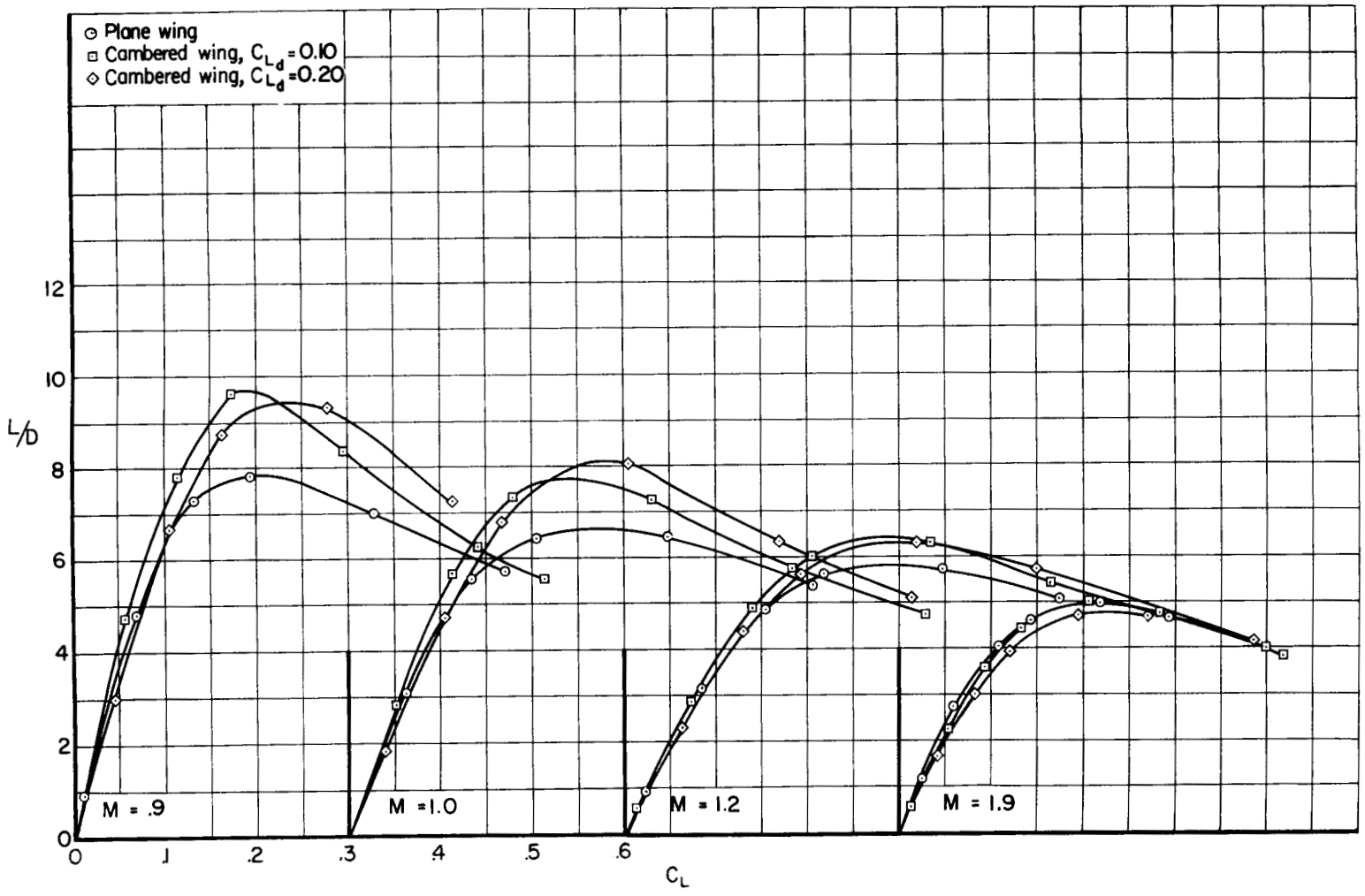

(a) Cambered over 10 percent of the local semispan.

Figure 7.- Effect of conical camber on the variation of lift-drag ratio with lift coefficient.

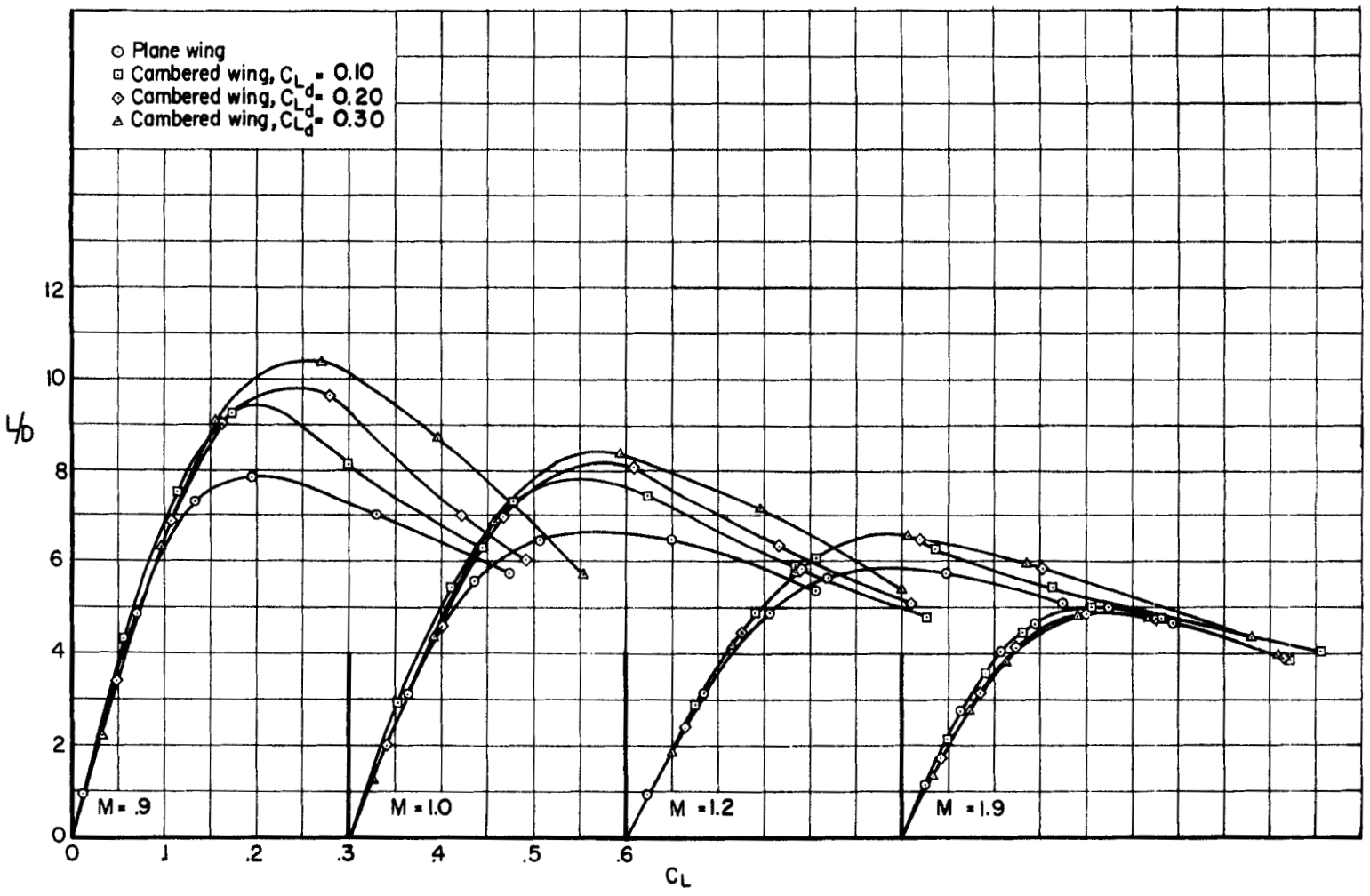

(b) Cambered over 15 percent of the local semispan.

Figure 7.- Concluded.

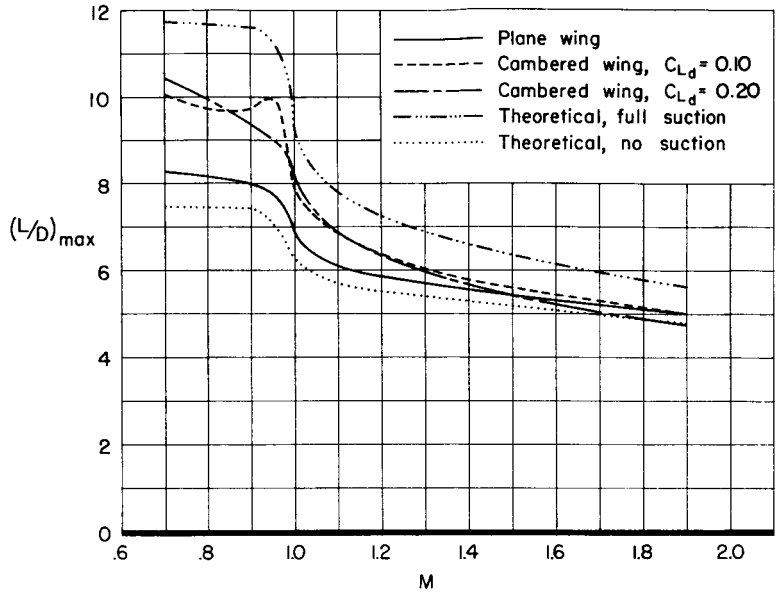

(a) Cambered over 10 percent of local semispan.

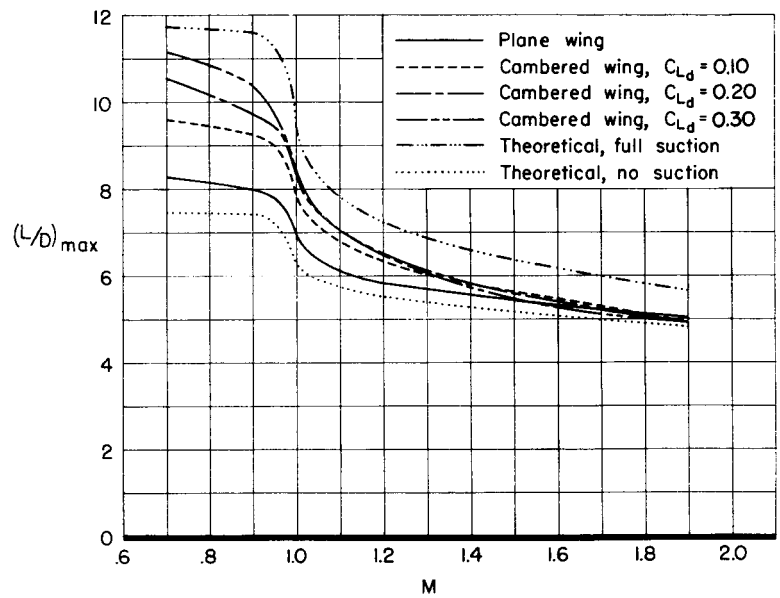

(b) Cambered over 15 percent of local semispan.

Figure 8.- Effect of conical camber on the variation of maximum lift-drag ratio with Mach number.

[redacted]

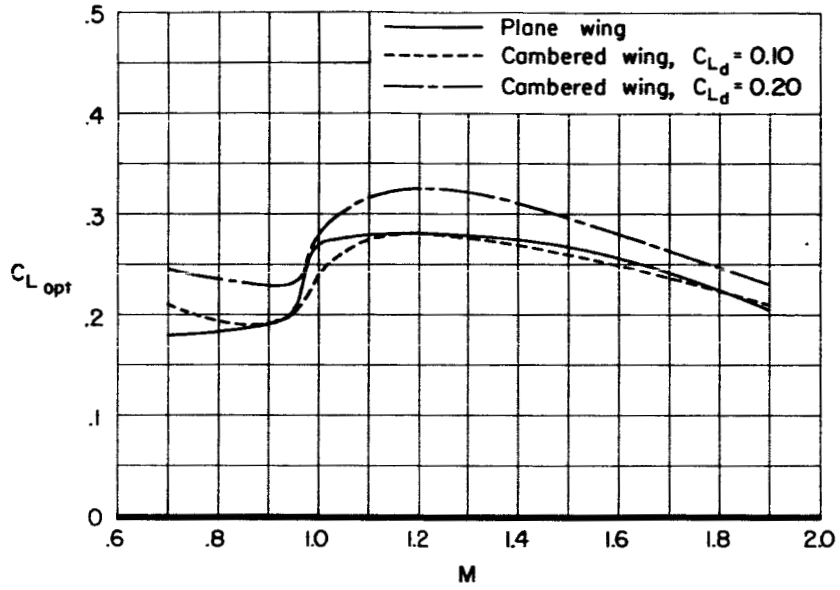

(a) Cambered over 10 percent of local semispan.

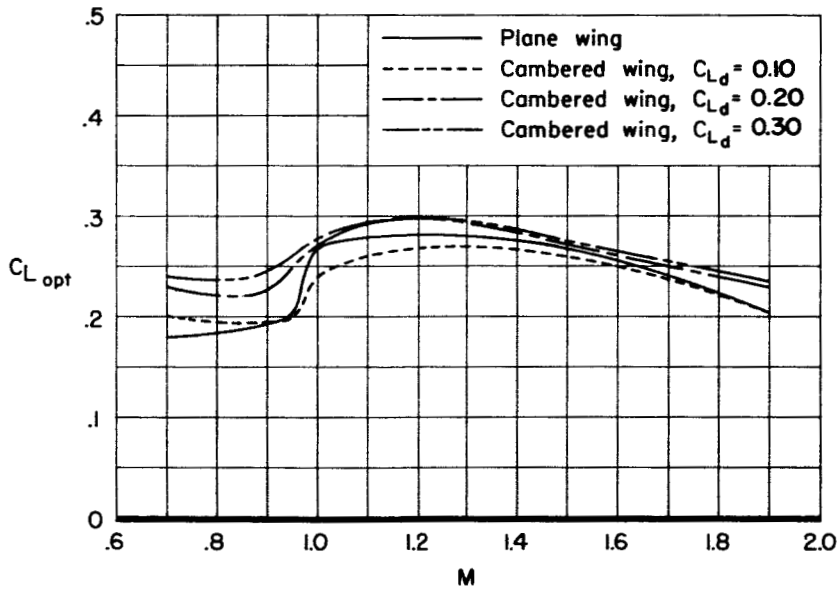

(b) Cambered over 15 percent of local semispan.

Figure 9.- Effect of conical camber on the variation of optimum lift coefficient with Mach number.

[redacted]

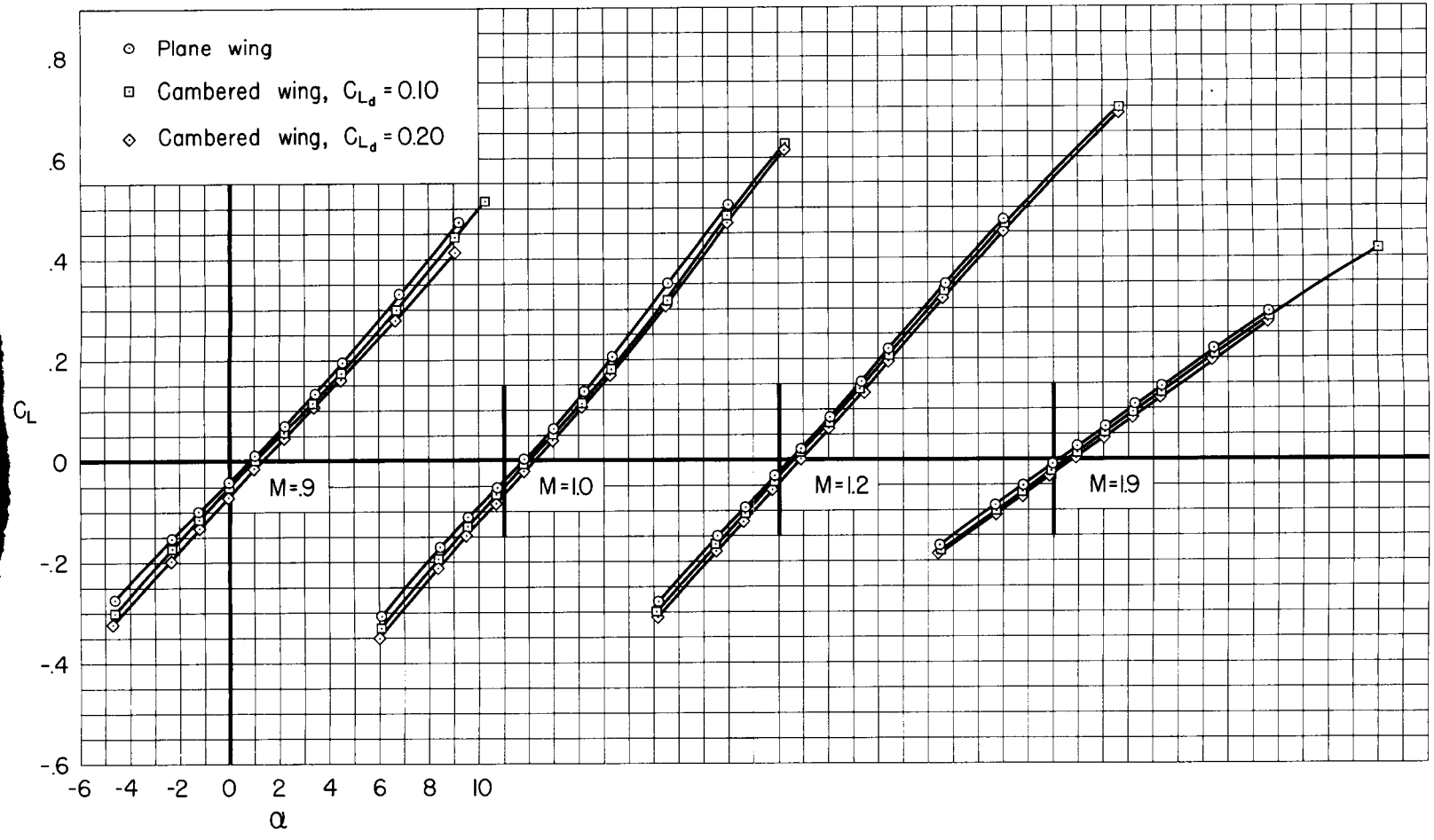

(a) Cambered over 10 percent of local semispan.

Figure 10.- Effect of conical camber on the variation of lift coefficient with angle of attack.

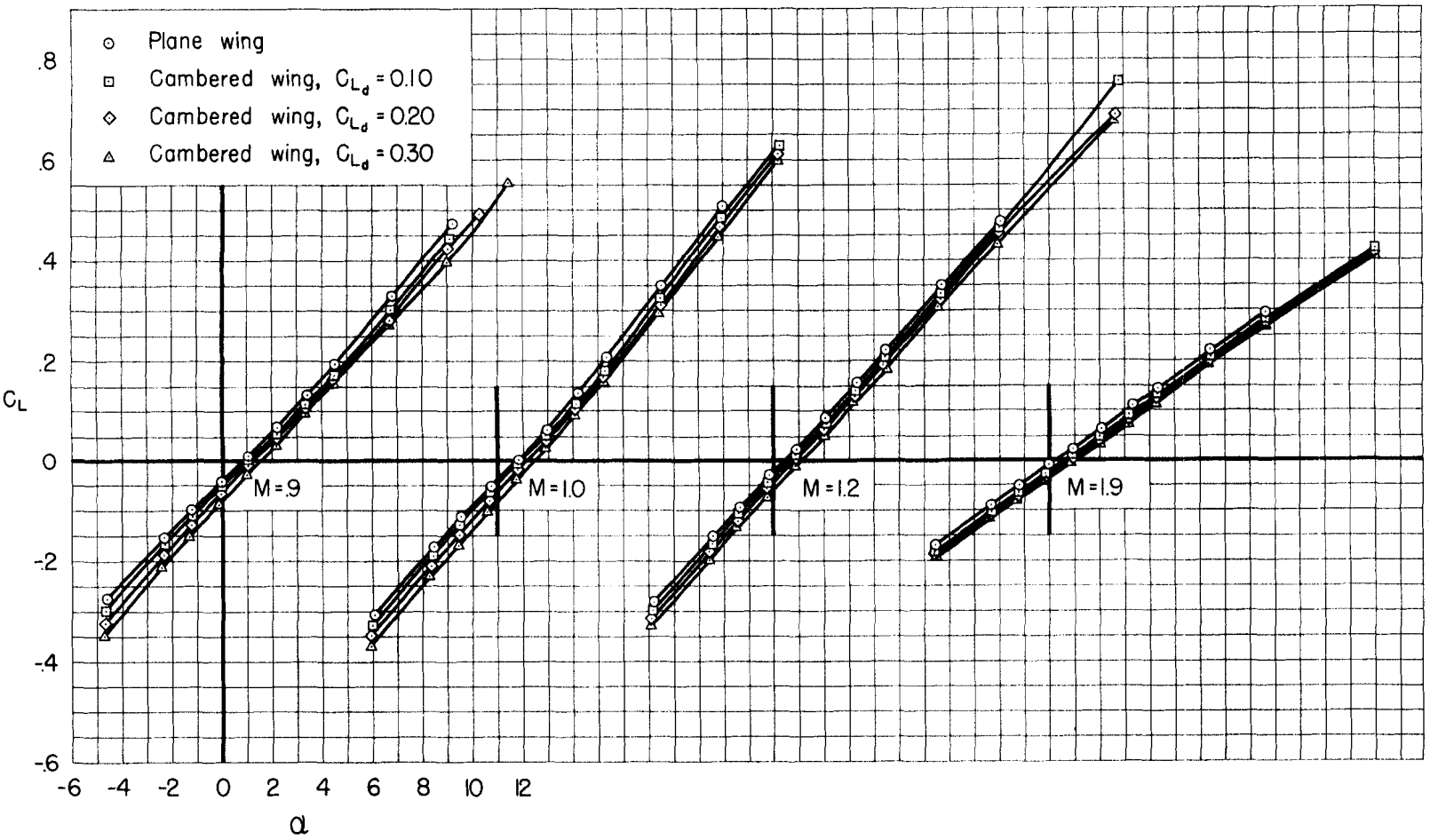

(b) Cambered over 15 percent of local semispan.

Figure 10.- Concluded.

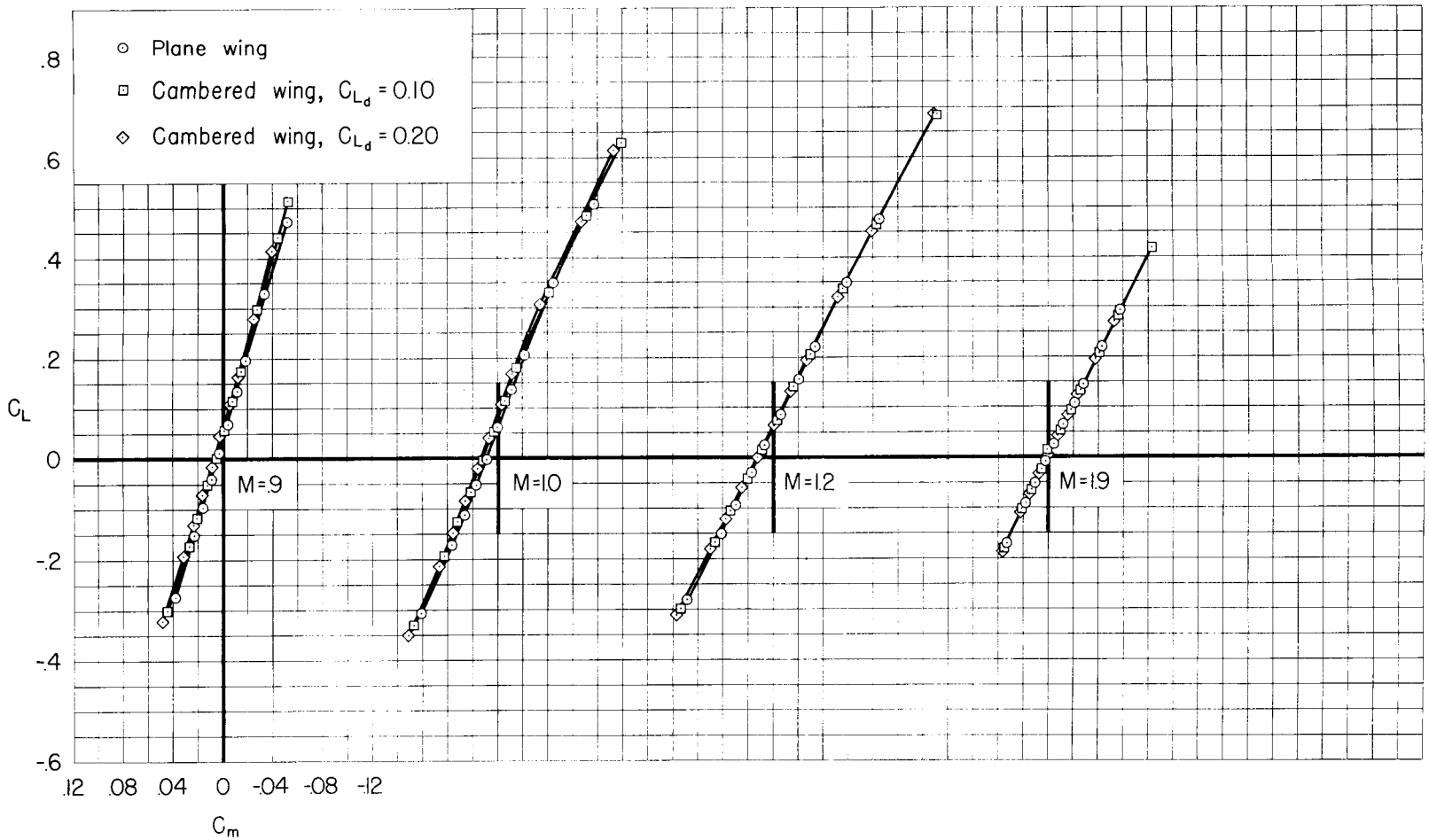

(a) Cambered over 10 percent of local semispan.

Figure 11.- Effect of conical camber on the variation of pitching moment with lift coefficient.

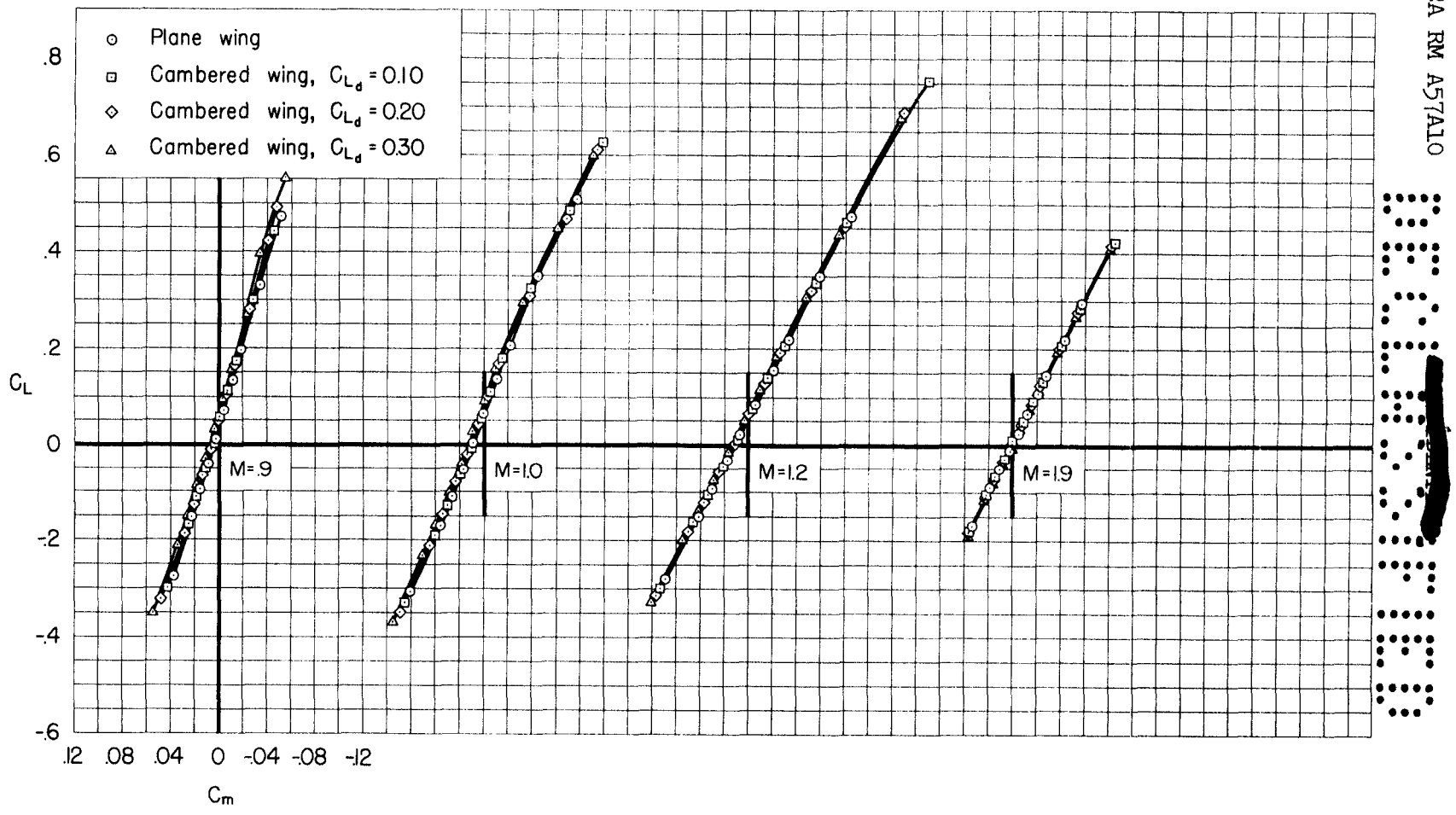

(b) Cambered over 15 percent of local semispan.

Figure 11.- Concluded.

[redacted]

7/66 26045

[redacted]